Journal of Advanced Research 39 (2022) 73–88

Contents lists available at ScienceDirect

Journal of Advanced Research

journal homepage: www.elsevier.com/locate/jare

Demystifying the long noncoding RNA landscape of small EVs derived from human mesenchymal stromal cells

Chien-Wei Lee [a,b,c], Yi-Fan Chen [d,e,f,g], Allen Wei-Ting Hsiao [h], Amanda Yu-Fan Wang [h], Oscar Yuan-Jie Shen [i], Belle Yu-Hsuan Wang [h], Lok Wai Cola Ho [j], Wei-Ting Lin [k], Chung Hang Jonathan Choi [j,l], Oscar Kuang-Sheng Lee [m,n,*]

[a] Department of Medicine Research, China Medical University Hospital, Taichung, Taiwan
[b] Institute for Tissue Engineering and Regenerative Medicine, The Chinese University of Hong Kong, Shatin, Hong Kong
[c] School of Biomedical Sciences, Faculty of Medicine, The Chinese University of Hong Kong, Shatin, Hong Kong
[d] The Ph.D. Program for Translational Medicine, College of Medical Science and Technology, Taipei Medical University, Taipei 11529, Taiwan
[e] Graduate Institute of Translational Medicine, College of Medical Science and Technology, Taipei Medical University, 11031 Taipei, Taiwan
[f] International Ph.D. Program for Translational Science, College of Medical Science and Technology, Taipei Medical University, 11031 Taipei, Taiwan
[g] Master Program in Clinical Genomics and Proteomics, School of Pharmacy, Taipei Medical University, Taipei, 11031, Taiwan
[h] Department of Orthopaedics and Traumatology, Faculty of Medicine, Prince of Wales Hospital, The Chinese University of Hong Kong, Shatin, Hong Kong
[i] Faculty of Medicine, The Chinese University of Hong Kong, Shatin, Hong Kong
[j] Department of Biomedical Engineering, The Chinese University of Hong Kong, Shatin, Hong Kong
[k] Doctoral Degree Program of Translational Medicine, National Yang Ming Chiao Tung University and Academia Sinica, Taiwan
[l] School of Life Sciences, The Chinese University of Hong Kong, Shatin, Hong Kong
[m] Institute of Clinical Medicine, National Yang Ming Chiao Tung University, Taipei, Taiwan
[n] Department of Orthopedics, China Medical University Hospital, Taichung, Taiwan

HIGHLIGHTS

- Cell-type specificity orchestrates the lncRNA signatures in small EVs (sEVs).
- LncRNA pattern in sEVs is distinct from their parental cells.
- MSC-sEV-specific and enriched lncRNAs were identified as medicinal signaling lncRNAs.
- lncRNA landscape of MSC-sEVs is responded to inflammatory cytokines.
- lncRNA-protein interactome associates with nuclear activity and chromatin remodeling.

GRAPHICAL ABSTRACT

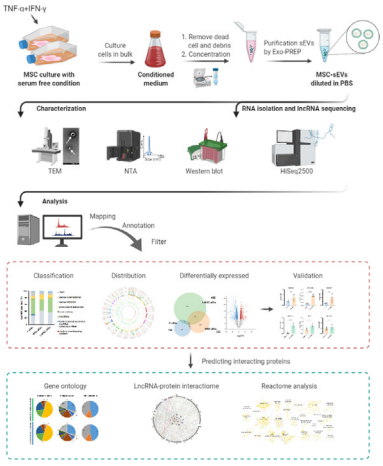

Peer review under responsibility of Cairo University.

* Corresponding author at: Institute of Clinical Medicine, National Yang Ming Chiao Tung University, Taipei, Taiwan. Department of Orthopedics, China Medical University Hospital, Taichung, Taiwan
E-mail address: oscarlee9203@gmail.com (O.K.-S. Lee).

https://doi.org/10.1016/j.jare.2021.11.003
2090-1232/

ARTICLE INFO

Article history:
Received 28 June 2021
Revised 1 November 2021
Accepted 7 November 2021
Available online 19 November 2021

Keywords:
MSCs
Exosomes
Cytokine priming
lncRNAs
protein–RNA interaction predictions

ABSTRACT

Introduction: The regenerative capacity of mesenchymal stromal cells or medicinal signaling cells (MSCs) is largely mediated by their secreted small extracellular vesicles (sEVs), and the therapeutic efficacy of sEVs can be enhanced by licensing approaches (e.g., cytokines, hypoxia, chemicals, and genetic modification). Noncoding RNAs within MSC-derived sEVs (MSC-sEVs) have been demonstrated to be responsible for tissue regeneration. However, unlike miRNA fingerprints, which have been explored, the landscape of long noncoding RNAs (lncRNAs) in MSC-sEVs remains to be described.

Objectives: To characterize lncRNA signatures in sEVs of human adipose-derived MSCs with or without inflammatory cytokine licensing and depict MSC-sEV-specific and MSC-enriched lncRNA repertoires.

Methods: sEVs were isolated from MSCs with or without TNF-α and IFN-γ (20 ng/mL) stimulation. High-throughput lncRNA sequencing and an *in silico* approach were employed to analyze the profile of lncRNAs in sEVs and predict lncRNA-protein interactomes.

Results: sEVs derived from human MSCs and fibroblasts carried a unique landscape of lncRNAs distinct from the lncRNAs inside these cells. Compared with fibroblast-derived sEVs (F-sEVs), 194 MSC-sEV-specific and 8 upregulated lncRNAs in MSC-sEVs were considered "medicinal signaling lncRNAs"; inflammatory cytokines upregulated 27 lncRNAs in MSC-sEVs, which were considered "licensing-responsive lncRNAs". Based on lncRNA-protein interactome prediction and enrichment analysis, we found that the proteins interacting with medicinal signaling lncRNAs or licensing-responsive lncRNAs have a tight interaction network involved in chromatin remodeling, SWI/SNF superfamily type complexes, and histone binding.

Conclusion: In summary, our study depicts the landscape of lncRNAs in MSC-sEVs and predicts their potential functions via the lncRNA-protein interactome. Elucidation of the lncRNA landscape of MSC-sEVs will facilitate defining the therapeutic potency of MSC-sEVs and the development of sEV-based therapeutics.

Introduction

Mesenchymal stromal cells, also known as medicinal signaling cells [1] (MSCs), have been heralded as a putative panacea for immunomodulation and regeneration medicine [2–6]. Over the last decade, applications of MSCs have shown satisfactory outcomes in numerous preclinical investigations and human clinical trials [7–9]. Moreover, MSC-sEVs have recently drawn enormous attention because of their broad therapeutic potential in various diseases, similar to their parental cells of origin [8,10], and most importantly, there have no associated practical safety issues [11].

sEVs, lipid bilayer particles < 200 nm in diameter, are released from budding membranes of multivesicular bodies in most cell types. sEVs play a crucial role in intercellular communication and homeostasis by horizontally transferring miRNAs, lncRNAs, tRNAs, mRNAs, genomic DNA, mitochondrial DNA, lipids, proteins, and even metabolites to recipient cells through plasma membrane fusion [12–16]. LncRNAs are defined as transcripts exceeding 200 nucleotides (nt) but not belonging to any other class of noncoding RNAs. LncRNAs have been implicated in diseases, cellular functions, and as potential therapeutics by regulating gene expression at the transcriptional and posttranscriptional levels via biological molecular interactions [17]. Recent reports have indicated that lncRNAs present in MSC-sEVs possess regenerative potential in wound healing [18], osteoarthritis [19], and acute myocardial infarction [20] through diverse mechanisms. However, these studies applied a candidate approach to select specific lncRNAs within MSC-sEVs and evaluated their therapeutic capability, and this approach may obscure/overlook the quantity variance and plenary effect of lncRNAs in MSC-sEVs. Rather than one individual molecule within the vesicles, the therapeutic ability of MSC-sEVs depends on the synergism of their intricate and numerous contents, which target different therapeutic pathways in recipient cells.

The concept of transplanted MSC adaptation to new environments [21] has been applied to enhance the regenerative efficacy of these cells *in vitro* for specific therapeutic applications. Enhancing the therapeutic ability of MSCs by genetic or culture conditions, which is also called licensing or priming, is an emerging strategy in the field of MSC-sEV-based therapy [4]. Inflammation is highly associated with tissue injury and diseases and can be either beneficial or deleterious to tissue regeneration [22]. The inflammatory cytokines TNF-α and IFN-γ stimulate MSCs *in vitro*, which partly mimics the *in vivo* environments of various diseases [23] and is reported to augment the immunomodulatory and tissue regenerative ability of MSC-sEVs [24–29]. Although the expression profiles of proteins and miRNAs in MSC-sEVs have been described and their functions in tissue regeneration have been annotated [24,30–34], the lncRNA landscape of MSC-sEVs remains largely undescribed. Before application in clinical therapies, it is a sine-qua-non to comprehensively and meticulously investigate lncRNAs within MSC-sEVs, including their favorable and putative undesirable side effects.

To fill this critical knowledge gap, the first goal of this study was to systematically describe the lncRNA landscape of sEVs derived from human adipose-derived MSCs and identify MSC-specific and MSC-enriched lncRNAs, which are defined as medicinal signaling lncRNAs. The second objective was to delineate licensing-responsive lncRNAs of MSC-sEVs under inflammatory stimulation. Cataloging medicinal signaling lncRNAs and licensing-responsive lncRNAs in sEVs derived from naïve MSCs and inflammation-licensed MSCs will have far-reaching implications in defining therapeutic sEVs and strengthen the fundamental understanding of MSCs for the development of next-generation MSC-based therapies.

Material and methods

Cell culture and characterization

Good Manufacturing Practices (GMP)-Grade human adipose-derived MSCs (Steminent Biotherapeutics Inc., Taiwan) were cul-

tured in MSC maintenance medium consisting of IMDM, 10% FBS (#10270106, Gibco®, Thermo Fisher Scientific, Waltham, MA, USA), 10 ng/mL bFGF (#233-FB, R&D Systems, Minneapolis, MN, USA) and 1% PSG (#10378016, Gibco®). Human skin fibroblasts (#GM08429, Coriell Institute, Camden, NJ, USA) were cultured in alpha MEM supplemented with 15% FBS and 1% PSG at a seeding density of 3000 cells/cm^2, and the cells were subcultured after reaching confluence. MSC characteristics were confirmed according to the minimal criteria defined by the International Society for Cell and Gene Therapy (ISCT) [35]. Surface markers were analyzed using a FACSAria Fusion Cell sorter and Cell Analyzer (BD Biosciences, San Jose, CA, USA). Primary antibodies for flow cytometry were as follows: anti-CD105, anti-CD90, anti-CD73, anti-CD34, anti-CD45 and anti-CD11b (#800505, #328107, #344015, #343607, #368511, #301309, BioLegend, San Diego, CA, USA; 1:100 dilution). Multidifferentiation capacities were assessed by alkaline phosphatase and Oil Red O, as previously described [9,36].

MSC sEV isolation and characterization

Cells were washed with PBS three times to remove the maintenance medium and FBS-derived exogenous EVs, and the cells were treated with or without 20 ng/mL TNF-α and 20 ng/mL IFN-γ (#210-TA, #285-IF, R&D Systems) for 48 h under serum-free conditions to avoid FBS-derived exogenous EV interference. The conditioned medium was centrifuged at 3000 × g for 20 min and filtered through 0.22-μm filters to remove detached cells and debris. The filtered conditioned medium was then concentrated using 30-kDa Vivaspin (#28–9323-61, GE Healthcare, Chicago, IL, USA) devices to an appropriate concentration at 4 °C. sEVs were then isolated from the concentrated conditioned medium using Exo-PREP (#HBM-EXP-C25, HansaBioMed Life Sciences Ltd, Tallinn, Estonia), resuspended in PBS and characterized according to suggestions from the International Society for Extracellular Vesicles [37,38].

Transmission electron microscopy (TEM)

The morphology of sEVs was observed by transmission electron microscopy (Hitachi H-7700, Tokyo, Japan). Twenty microliters of sEVs was dropped onto a carbon-coated formvar film (#FC200Cu100, EM Resolution, South Yorkshire, United Kingdom) for 15 min and then fixed with 1% glutaraldehyde (#G6257, Sigma-Aldrich, St. Louis, MO, USA) for 15 min. The grid was washed with ddH2O twice and stained with 2% uranyl acetate (#22400, Electron Microscope Science, Hatfield, PA, USA). After washing with ddH2O, the sEVs were air-dried and imaged with H-7700 operating at 100 keV.

Nanoparticle tracking analysis (NTA)

The number and size distribution of sEVs was measured using NTA version NTA 3.1 Build 3.1.45 (Nanosight NS300, Malvern Panalytical, Malvern, United Kingdom). For measurement, the instrument preacquisition parameters were set to 24 °C, with a slider gain of 15, a slider shutter of 165, and a frame rate of 25 frames per second (fps). sEVs were diluted in various amounts of filtered PBS to determine the optimal concentration for analysis. These measurements were analyzed by dedicated NanoSight NTA software, with a detection threshold of 2, autoblur size, and a maximum jump distance of 14.2 pixels. The mean and mode diameter and the concentrations of sEVs were recorded.

Western blotting

MSCs and sEVs were lysed in RIPA buffer (#ab156034, Abcam, Cambridge, UK) with 1X protease/phosphatase inhibitor (#1861281, Thermo Fisher Scientific), and the protein content was measured by BCA analysis (#23225, Thermo Fisher Scientific). For western blotting, protein samples were separated on polyacrylamide gels and transferred to PVDF membranes (#IPVH00010, Merck Millipore, Massachusetts, USA). The membranes were incubated with 5% bovine serum albumin (#A9647, Sigma-Aldrich) followed by probing with primary antibodies overnight at 4 °C and then staining with HRP-conjugated secondary antibodies for 1 h at room temperature. A chemiluminescent substrate (#34095, Thermo Fisher Scientific) was added to the membranes, and images were acquired with the ChemiDoc MP imaging system (Bio-Rad, Hercules, CA, USA). The following primary antibodies were used: CD63 antibody (#NBP2-42225ss, Novus Biologicals, Centennial, USA), CD9 antibody (#10626D, Invitrogen, Carlsbad, CA, USA), and β-actin antibody (#sc-47778, Santa Cruz).

RNA isolation, RNA sequencing and quantitative real-time PCR

RNA was extracted by TRIzol (#15596018, Invitrogen). The RNA content and quality were determined by a NanoDrop (Thermo Fisher Scientific) and an Agilent Bioanalyzer 2100 system (Agilent Technologies, CA, USA). Samples with an OD260/OD230 > 1.8, OD260/OD280 ratio of approximately 2.0, and RNA integrity ≥ eight were subjected to RNA sequencing using an Illumina HiSeq 2500. For quantitative PCR, cDNA was transcribed by a High-Capacity cDNA Reverse Transcription Kit (#4368814, Applied Biosystems, Foster City, CA, USA). Quantitative real-time PCR was performed by using a QuantStudio™ 7 Flex Real-Time PCR System (Applied Biosystems, Foster City, CA, USA) with Fast SYBR™ Green Master Mix (#4385612, Thermo Fisher Scientific). The primers are listed in Table S1.

LncRNA expression analysis

Quality control of the RNA sequencing data was conducted using FastQC software (http://www.bioinformatics.babraham.ac.uk/projects/fastqc/, version 0.11.7). Ensembl Automatic Gene Annotation System (http://www.ensemble.org) and GENCODE version 27 [39] were used to annotate and evaluate lncRNA expression. Transcripts with<200 base pairs were filtered out. The transcript abundance of lncRNAs between each sample was normalized with transcripts per million (TPM). We conducted differential expression (DE) analysis with the limma package [40] (version 3.42.2; http://bioconductor.org/packages/release/bioc/html/limma.html) in R 3.6.3 (RStudio Team (2020)). RStudio: Integrated Development for R. RStudio, Inc., Boston, MA URL http://www.rstudio.com/) to identify DE lncRNAs according to thresholds of the absolute value of log2-fold-change (log2 FC) > 1 and a P value < 0.05. The volcano plot of DE lncRNAs was generated with GraphPad Prism 8.

LncRNA-protein interactome predictions

To predict lncRNA-protein interactions, we used the computationally expensive protein–RNA interaction prediction method catRAPID [41] with the large database RNAct (https://rnact.crg.eu/). The catRAPID algorithm is based on X-ray and nuclear magnetic resonance (NMR) structures to estimate the interaction propensity of RNA-protein pairs through van der Waals forces, secondary structures, and hydrogen bonding. Briefly, upregulated DE lncRNAs in datasets (medicinal signaling lncRNAs and licensing-responsive lncRNAs) were loaded into RNAct to predict interacting proteins, and the predicted target proteins were used to generate protein reactomes by using the Reactome database (version 75;

https://reactome.org/) [42]. Functions of the lncRNA-protein interactome (top 100 predicted interacting proteins of each lncRNA) were analyzed by the PANTHER classification system [43] (version 16.0, https://www.pantherdb.org). The interaction network of the lncRNA-protein interactome (top 30 predicted interacting proteins of each lncRNA) was analyzed with GeneMANIA (http://genemania.org) [44].

Statistical analysis

Quantitative data were analyzed as the mean ± SD in the histogram with the data point. Statistical analyses were performed using GraphPad Prism 8 (GraphPad Software, La Jolla, CA, USA) with one-way ANOVA with post hoc Tukey HSD, unpaired Student's *t*-test, and multiple t-tests methods depending on the experimental design. A value of $P < 0.05$ was considered statistically significant.

Availability of data

All data of this study are included in this published article and are available from the corresponding author upon request. The RNA-Seq dataset supporting the conclusions of this article is available in the GEO database, GSM921009, GSM921016, GSM921023, GSM921030, GSM921038, GSM921046, GSM920963, GSM920978, GSM920994, GSM921002, GSM2049181, and GSM2049182 [45,46].

Results

Characterization of sEVs derived from human naïve and licensed MSCs

Human adipose-derived MSCs, which have typical spindle-like morphology, surface phenotypes, and multidifferentiation capacities, were used in this study (Figure S1). Fig. 1 shows the graphic flowchart of this study. MSCs were treated with TNF-α and IFN-γ for 48 h to investigate the effects of inflammatory stimulation on MSCs. Neither TNF-α nor IFN-γ or cotreatment altered the morphology (Fig. 2A), viability (Fig. 2B), or typical surface markers (Fig. 2C) of MSCs compared with naïve MSCs. However, TNF-α and cotreatment did enlarge cell size, as measured by forward scatter in flow cytometry (Fig. 2D). IFN-γ, but not TNF-α, partially enhanced expression of anti-inflammatory cytokines, including IDO and CXCL9. Cotreatment significantly upregulated anti-inflammatory cytokines, suggesting a synergistic effect of TNF-α and IFN-γ on MSC immunomodulatory ability (Fig. 2E).

Subsequently, we isolated sEVs from naïve MSCs and TNF-α and IFN-γ cotreated MSCs (licensed MSCs, L-MSCs) (Fig. 1). TEM analysis revealed that both naïve MSC-sEVs and L-MSC-sEVs had similar oval membranous vesicle morphology (Fig. 3A). The most well-known sEV surface signatures are endosome-specific tetraspanins (CD9 and CD63), which are involved in the production, selective uptake, EV heterogeneity and vesicular component sorting [47,48]. The MSC-sEVs and L-MSC-sEVs we examined expressed the typical characteristic markers CD63 and CD9 (Fig. 3B). In addition, hydrodynamic particle size distribution and yields were measured by NTA, with no significant difference in the distribution or average hydrodynamic particle size between MSC-sEVs and L-MSC-sEVs (Fig. 3C-D). The prominent peaks in particle size were 162 ± 23 nm and 150 ± 18 nm in MSC-sEVs and L-MSC-sEVs, respectively (Fig. 3E). The total quantity and space–time yield of sEVs were increased by 76.7% and 86.7%, respectively, suggesting that licensing enhances MSC vesiculation (Fig. 3F-G). Overall, total RNA and protein contents were not altered by licensing (Fig. 3H-I). Our results indicate that both naïve MSCs and L-MSCs liberate sEVs, though L-MSCs produced more sEVs than naïve MSCs. Our results suggest that licensing MSCs with TNF-α and IFN-γ enhances sEV production without affecting morphology.

Investigation of lncRNAs in sEVs derived from human fibroblasts, MSCs and L-MSCs

We applied high-throughput lncRNA sequencing to comprehensively analyze lncRNA signatures of sEVs from naïve MSCs and L-MSCs without bias and compared them with those from human F-sEVs obtained from public databases [45,46]. The total lncRNA counts in both MSC- and L-MSC-sEVs were higher than those in F-sEVs; the total abundance of lncRNAs in L-MSC-sEVs was higher than that in MSC-sEVs (Fig. 4A). The distribution of transcripts per kilobase million (TPM) values was significantly distinct in each group. The TPM distribution of F-sEVs was higher than that of both MSC-sEV groups (Fig. 4B), and licensing reduced the TPM distribution, suggesting an increase in low-abundance lncRNAs in L-MSC-sEVs (Fig. 4B). The length distribution ratio of lncRNAs is depicted in Fig. 4C. There was no significant difference among the groups (Table S2). The two major ranges of lncRNAs were 100,000 to 10,000 nt and 5,000 to 1,000 nt in all groups. In detail, lncRNAs in naïve MSC-sEVs ranged from 74 to 440,879 nt in length, those in licensed MSC-sEVs ranged from 74 to 475,377 nt in length, and those in F-sEVs ranged from 93 to 440,879 nt. We classified the sEV-lncRNAs into nine subclasses according to the biogenesis and structure of lncRNAs [49] (Fig. 4D), with no significant difference among all groups (Table S3). The primary types of lncRNAs in sEVs were antisense RNA and lincRNA, together accounting for 74%-78% of all lncRNAs in all groups.

To investigate the distribution of the sEV lncRNA reference genome, we visualized the chromosomal distribution of lncRNAs by Circos (Fig. 4E, left panel). Most lncRNAs in sEVs are transcribed from chromosomes 1 and 17 (Fig. 4E right panel). Widespread lncRNA distribution along all chromosomes and the distinct distribution within a chromosome between three groups indicated that the lncRNAs identified were not transcriptional noise (Fig. 4E, left panel). In general, the differences in TPM distribution, length, types, and chromosome distribution of lncRNAs indicated that both lineage specificity and unique microenvironments govern lncRNA proportions in sEVs.

lncRNA landscape in sEVs derived from human fibroblasts and MSCs

Through correlation coefficient analysis, we found that the lncRNAs of MSC-sEVs were distinct from those of F-sEVs; surprisingly, lncRNAs of MSC-sEVs and L-MSC-sEVs correlated highly (Fig. 5A). A total of 132, 233, and 496 lncRNAs were identified in F-sEVs, MSC-sEVs, and L-MSC-sEVs, respectively. Comparing F-sEVs and MSC-sEVs, 93 lncRNAs were expressed only in F-sEVs, and 194 lncRNAs were only present in MSC-sEVs; only 39 lncRNAs were identified in both sample pools. Because MSC-sEVs, but not F-sEVs, possess therapeutic potential, 194 MSC-specific lncRNAs were considered potential medicinal signaling lncRNAs. Overall, 389 lncRNAs were gained and 129 lncRNAs lost after licensing compared with MSC-sEVs. Among the three groups, 89 lncRNAs were expressed exclusively in F-sEVs, 121 lncRNAs were only expressed in MSC-sEVs, and 385 were newly observed in L-MSC-sEVs. Only 34 lncRNAs were identified across the three sample pools (Fig. 5B). These results suggest that cell-type specificity orchestrates the disparate lncRNA signatures in sEVs for unique sEV-mediated intercellular communication between various cell types. Although the lncRNA profile of sEVs responds to microenvironmental stimulation, lineage specificity might restrict changes.

The ranking of lncRNA expression levels in sEVs was ordered according to TPM value, and the top 10 enriched lncRNAs of the

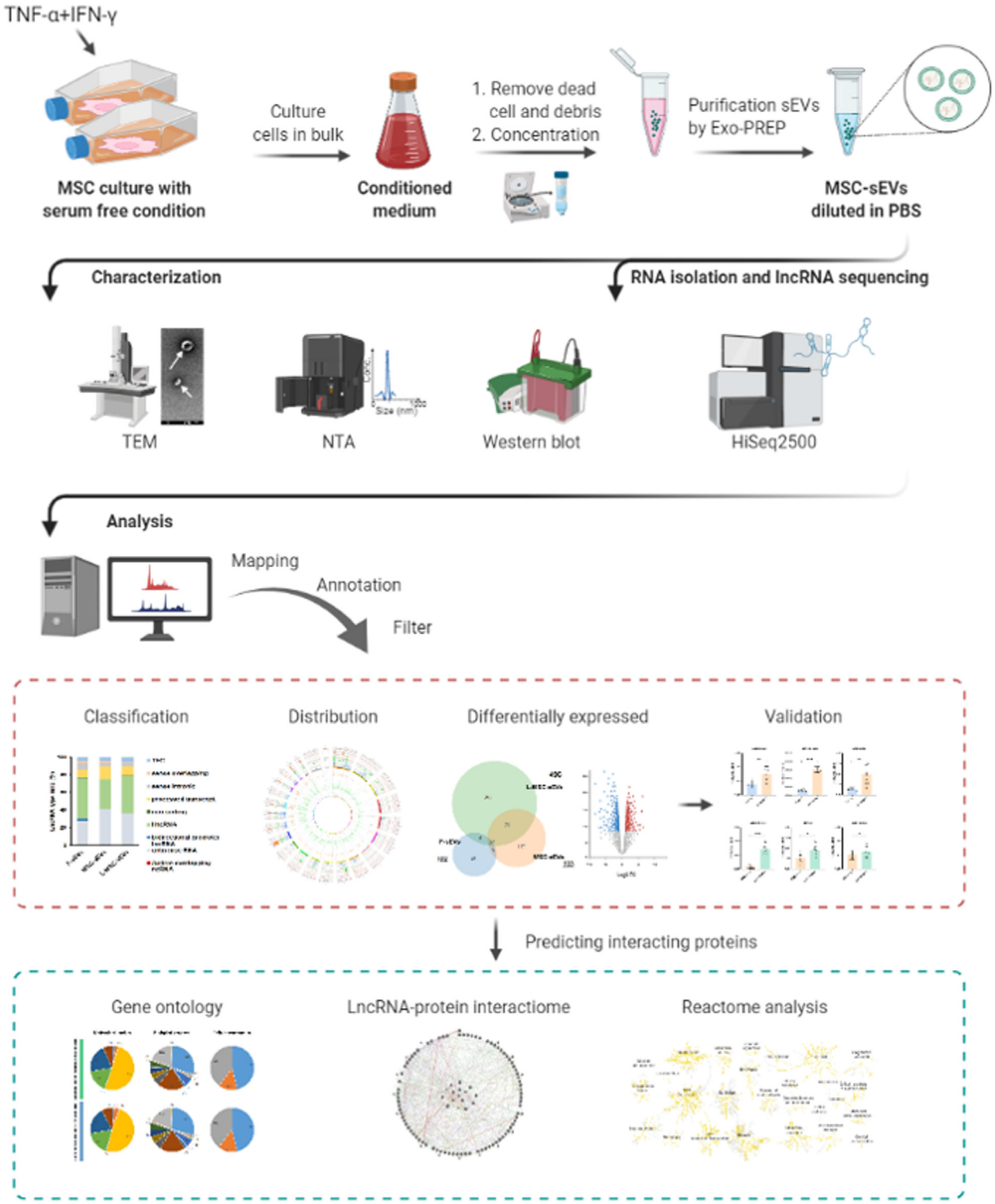

Fig. 1. Schematic representation of human adipose MSC-sEV stimulation, isolation, characterization, and MSC-sEV lncRNA analysis. Human MSCs were stimulated with TNF-α and IFN-γ for 48 h under serum-free conditions. After removing debris and concentrating the conditioned medium, EVs released by naïve MSCs and licensed MSCs (MSC-sEVs and L-MSC sEVs) were isolated by Exo-PREP. The EVs were characterized by nanoparticle tracking analysis (NTA), transmission electron microscopy (TEM) and western blotting. High-throughput RNA sequencing was used to identify expression profiles of lncRNAs in EVs. Quality control of the RNA sequencing data was conducted using FastQC software. High-quality lncRNAs were obtained by mapping, annotation and filtering. LncRNA classification and distribution were analyzed by bioinformatics tools. Differential expression (DE) analysis was conducted, followed by quantitative PCR-based biological validation. LncRNA-interacting proteins were identified by a computational prediction method, catRAPID. The gene ontology, protein interactome and reactome of lncRNA-interacting proteins were further deciphered using online tools, the PANTHER classification system, GeneMANIA and Reactome.

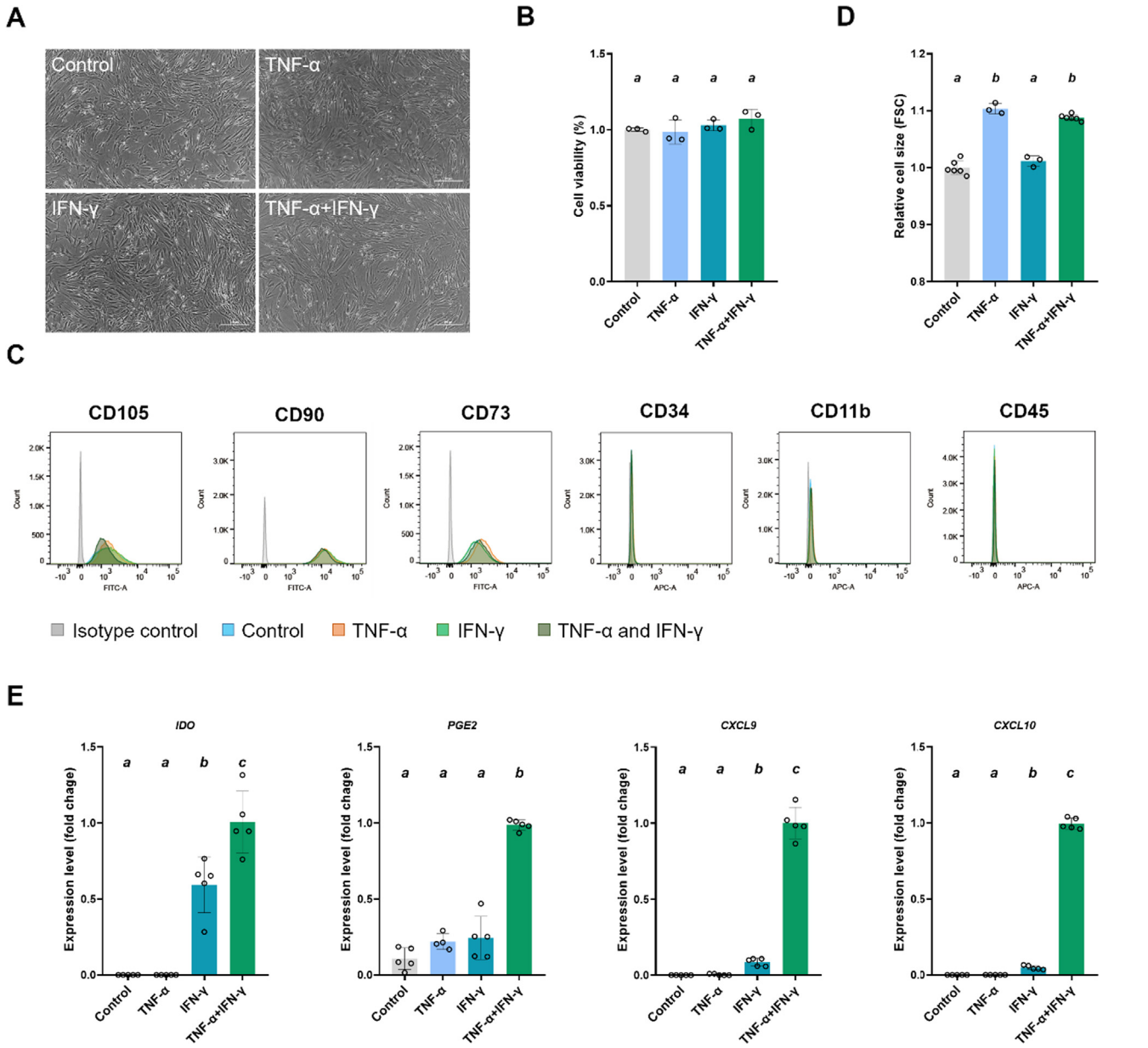

Fig. 2. Inflammatory cytokines stimulate human adipose-derived MSCs. MSCs were treated with TNF-α and IFN-γ for 48 h under serum-free conditions. (A) Representative morphology. Scale bar, 100 μm. (B) Cell viability was measured by the CCK-8 assay (n = 3); results were normalized to the control group. (C-D) MSC surface phenotype (C) and relative cell size (D) were determined by flow cytometry (n = 3 to 6). (E) Expression levels of anti-inflammatory genes were measured by real-time PCR (n = 5); results were normalized to the TNF-α and IFN-γ cotreatment group because some genes were undetectable in the control group. TNF-α, 20 ng/mL and IFN-γ, 20 ng/mL. Results are shown as the means ± SD. Statistical analyses were performed using ANOVA with post hoc Tukey's HSD in multiple comparisons. Means not sharing any letters are significantly different ($P < 0.05$).

three groups are listed in Tables 1–3. The top 10 enriched lncRNAs in sEVs accounted for the vast majority in sEVs in each group, indicating that most lncRNAs in sEVs are present at a low level. Interestingly, the top 10 expressed lncRNAs in the three groups highly overlapped (Fig. 5C). The abundance of each enriched lncRNA in F-sEVs was relatively average compared with those of MSC-sEVs and L-MSC-sEVs. LncRNA AC051619.8, with the highest abundance in both MSC-sEVs and L-MSC-sEVs, accounted for 69.57% and 98.28% of all lncRNAs, respectively, though it comprised only 0.8% of lncRNAs in F-sEVs. Such extreme expression of AC051619.8 in both MSC-sEVs and L-MSC-sEVs explains the high correlation coefficients between the two groups. On the other hand, several enriched lncRNAs in MSC-sEVs were not exclusive. For instance, FP236383.3, FP236383.2, and AD000090.1 were enriched in both MSC-sEVs and F-sEVs, suggesting that they are nonlineage-specific lncRNAs.

Compared with F-sEVs, the top 10 new loading lncRNAs in MSC-sEVs, such as LINC00623, LINC00317 and SNHG20, compared with F-sEVs are shown in Fig. 5D. Fig. 5E illustrates the top 10 newly loaded lncRNAs after licensing, such as MINCR, TTTY19, and AC087897.2. The details of the top 10 newly loaded lncRNAs of the two datasets are given in Tables S4 and S5. Interestingly, increasing the TPM cutoff value to reduce potential sequencing noise between samples dramatically decreased the numbers of identified lncRNAs in MSC-sEVs (70.4% decrease) and L-MSC-sEVs (88.1% decrease), indicating that most lncRNAs in MSC-sEVs are expressed at low abundance (Fig. 5F). As we identified more lncRNAs in L-MSC-sEVs than in MSC-sEVs (Fig. 5B), licensing might

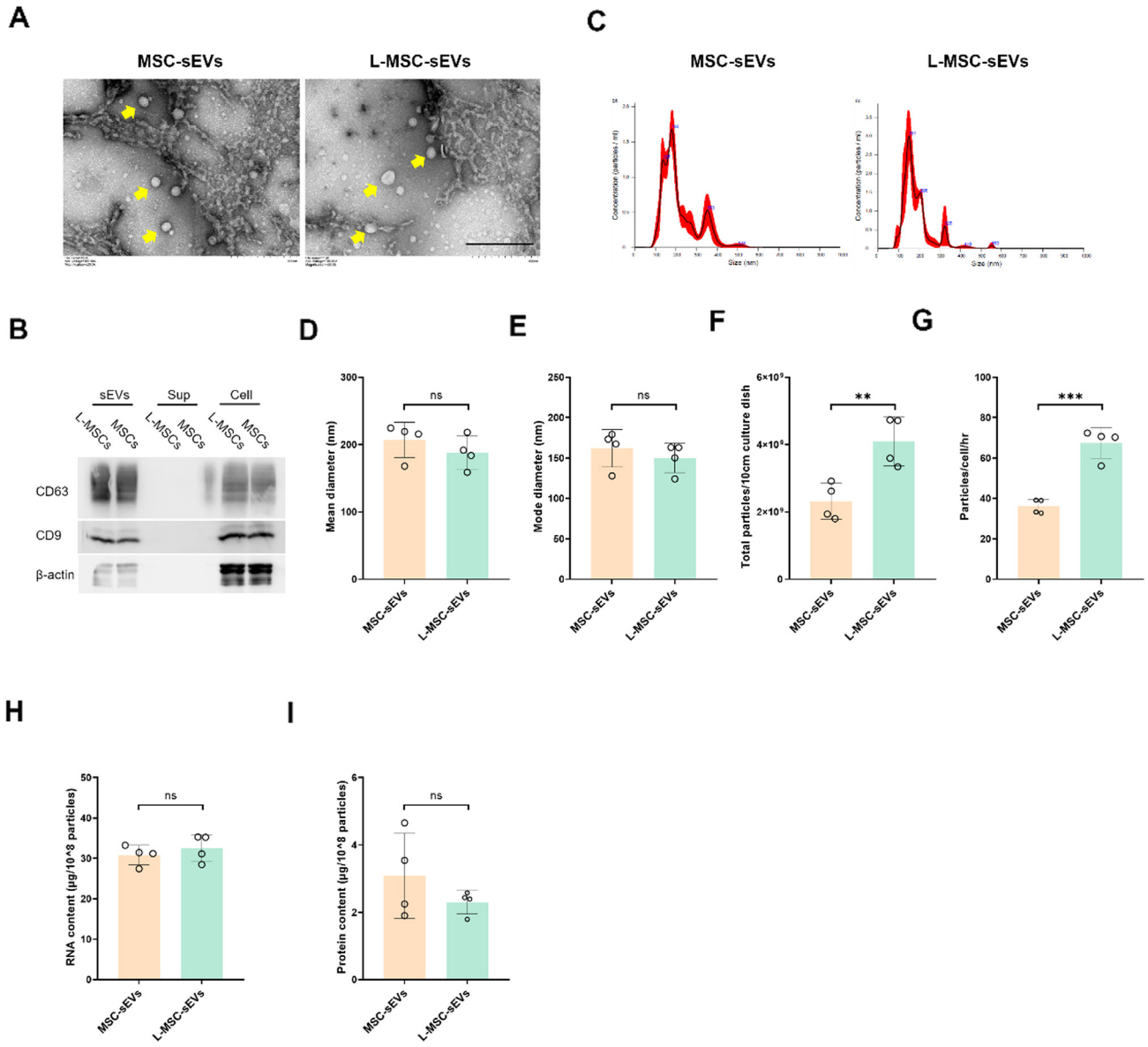

Fig. 3. Characterization of sEVs derived from naïve MSCs and licensed MSCs. (A) Transmission electron micrographs of isolated sEVs. Scale bar at 500 nm. Arrow indicates sEVs. (B) Western blotting analysis showed expression of the typical sEV markers CD63 and CD9 in sEVs. (C-E) NTA revealed the distribution (C), average hydrodynamic mean (D) and mode diameter (E) of sEVs (n = 4). (F-G) The total quantity of sEVs from 10 cm culture dishes (F) and space–time yield of sEVs (G). The concentration of sEVs was normalized to the cell number and induction period (n = 4). (H-I) The RNA and protein content in sEVs (n = 4). Results are shown as means ± SD with the data points. Statistical analyses were performed using Student's *t*-test. (*P < 0.05, **P < 0.01, *** P < 0.001; ns, not significant).

increase the heterogeneity of sEV lncRNAs by altering newly loaded lncRNAs with low abundance.

To identify potential medicinal signaling lncRNAs and licensing-responsive lncRNAs, we performed DE analysis between two datasets: (I) MSC-sEVs and F-sEVs and (II) MSC-sEVs and L-MSC-sEVs. A total of 224 and 55 lncRNAs were found to be significantly different in MSC-sEVs vs. F-sEVs and in MSC-sEVs vs. L-MSC-sEVs, respectively (Fig. 5G-H). We detected 224 DE lncRNAs in MSC-sEVs through comparison with F-sEVs. Among them, 8 upregulated DE lncRNAs were considered a cluster of medicinal signaling lncRNAs (fold change > 2 and P value < 0.05) (Fig. 5G). For instance, lncRNA LINC00623 was an upregulated DE lncRNA in MSC-sEVs and also the most enriched new loading lncRNA (Fig. 5D). LINC00623 has been reported to ameliorate osteoarthritis [50], indicating medicinal signaling potential. Additionally, we found 54 licensing-responsive lncRNAs, including 27 DE upregulated and 27 downregulated DE lncRNAs, in L-MSC-sEVs (Fig. 5H). The lncRNA MINCR, upregulated by licensing, was also the top 1 newly expressed loading lncRNA in L-MSC-sEVs; it has been reported to promote proliferation and migration by activating Wnt/β-catenin signaling [51–53]. The top 20 DE lncRNAs between MSC-sEVs vs. F-sEVs and MSC-sEVs vs. L-MSC-sEVs are listed in Tables S6 and S7, respectively. To verify the accuracy of the lncRNA sequencing data, we conducted quantitative PCR on randomly selected DE lncRNAs from the two datasets. Consistent with the sequencing results, quantitative PCR showed that LINC00623, ZNF436-AS1 and LINC00637 were more highly expressed in MSC-sEVs than in F-sEVs (Fig. 5I) and that AC051619.8 and MINCR, but not AC10967.2, were increased in L-MSC-sEVs compared with MSC-sEVs (Fig. 5J).

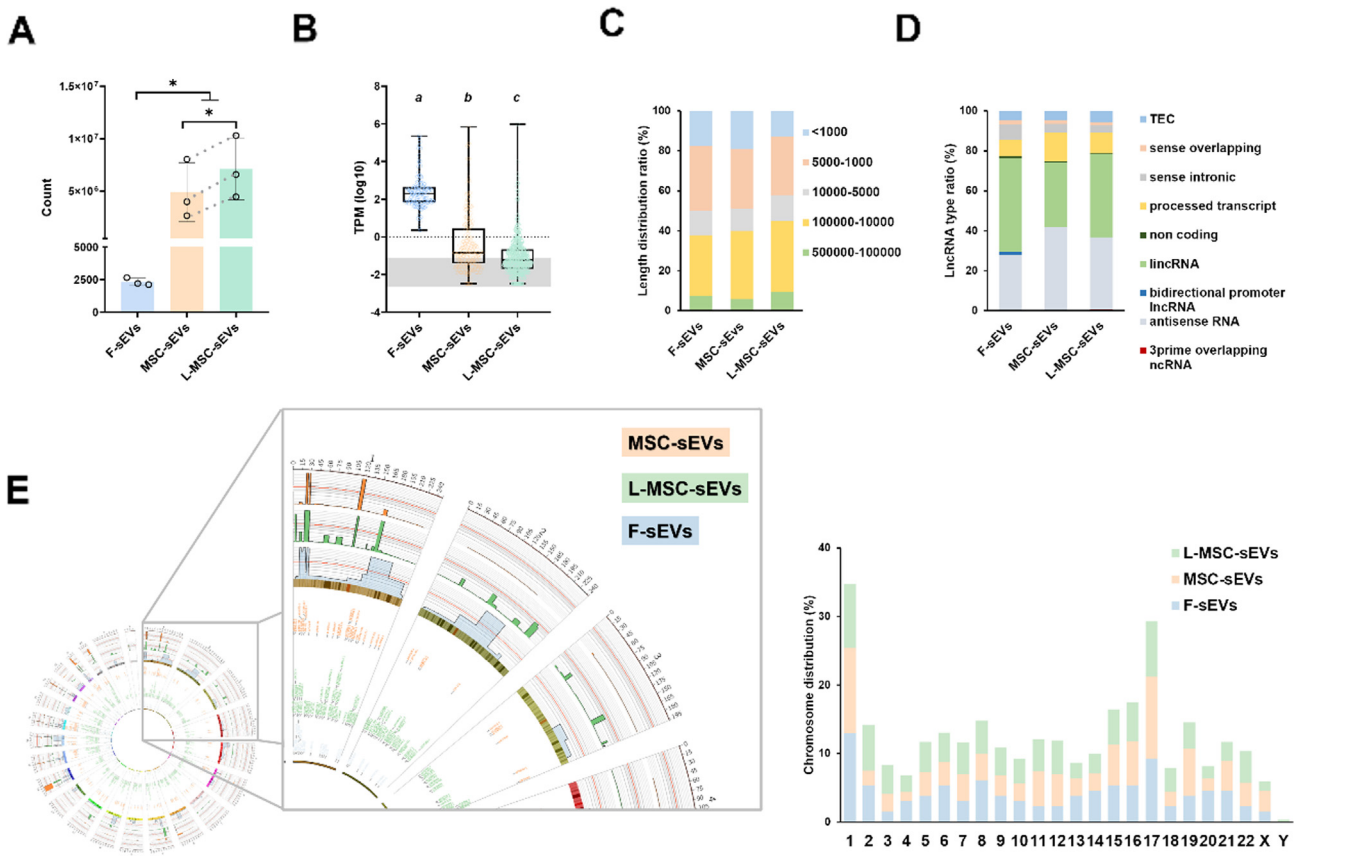

Fig. 4. Characteristics of lncRNAs from human MSC-sEV. (TPM cutoff > 0). (A) Total counts of lncRNAs in F-sEVs, MSCs-sEVs and L-MSC-sEVs (n = 3). (B) TPM distribution of all identified lncRNAs. (C) Length distribution of lncRNAs. (D) Classification of lncRNAs in MSC-sEVs into nine categories. (E) Visualized chromosomal distribution of lncRNAs in sEVs by using Circos. The outer ring represents lncRNAs labeled with chromosome number and position. Orange, green and blue circles show the distribution of identified lncRNAs in MSC-sEVs, L-MSC-sEVs and F-sEVs, respectively. The right histogram reveals the percentage of chromosome distribution of lncRNAs in the three groups. TPM cutoff > 0. Statistical analyses were performed by Student's *t*-test for panel A (*P < 0.05, **P < 0.01, *** P < 0.001; ns, not significant) by one-way ANOVA with post hoc Tukey's HSD in multiple comparisons. Means not sharing any letters are significantly different (P < 0.05).

The MSC-sEV lncRNA-protein interactome

The field of lncRNA research is still in its infancy, and most of the lncRNAs identified in this study have not yet been annotated. Because MSC-sEV lncRNAs are unlikely to regulate recipient genes in a *cis*-acting manner [54], i.e., regulating transcription of neighboring mRNAs at loci where they are transcribed, we sought to gain insight into the function of MSC-sEV lncRNAs through interacting proteins. To investigate medicinal signaling lncRNA- and licensing-responsive lncRNA-protein interactomes, we predicted interacting proteins of the upregulated DE lncRNAs in the two datasets using catRAPID in conjunction with the RNAct database. By estimating the interaction propensity of RNA-protein pairs through van der Waals forces, secondary structures, and hydrogen bonding contributions, a total of 301 and 452 proteins are predicted to interact with medicinal signaling lncRNAs and licensing-responsive lncRNAs, respectively; 251 predicted proteins were found in both sample pools (Fig. 6A). The details of the predicted proteins are provided in Supplemental material 1–3).

To delineate categories of the lncRNA-protein interactome, we performed Gene Ontology network analysis to decipher biological processes, molecular functions and cellular components in which medicinal signaling lncRNAs and licensing-responsive lncRNAs are implicated. Both medicinal signaling lncRNA- and licensing-responsive lncRNA-protein interactomes were enriched with similar annotations (Fig. 6B). Regarding the above GO categories, both interactomes were significantly associated with terms including binding and catalytic activity, cellular processes, and cellular anatomical entities. Protein-protein interaction network analysis revealed a complex and highly connected cluster in both interactomes (Fig. 6C-D). Functional enrichment analysis of both interactomes showed that the most significantly enriched pathways involve chromatin remodeling, the SWI/SNF superfamily type complex, and histone binding (Fig. 6C-D). We subsequently analyzed functional enrichment according to the entity reaction network, and coverage of both medicinal signaling lncRNA- and licensing-responsive lncRNA-protein interactomes occurred throughout the whole reactome, including chromatin organization (Fig. 6E-F). Our results indicate that medicinal signaling lncRNAs and licensing-responsive lncRNAs might interact with chromatin remodeling proteins to override the regulatory machinery in the nucleus of recipient cells.

Unique lncRNA signatures across sEVs and parental cells

sEVs exhibit lineage specificity that is dependent on cell origin, and we thus hypothesized that the lncRNA profile of sEVs is equal to that of their parental cells. The distribution of TPM between F-sEVs and fibroblasts was significantly distinctive, and the same was observed between MSC-sEVs and MSCs (Fig. 7A). sEVs contained shorter lncRNAs (<1000 bp) compared with their parental cells), whereas longer lncRNAs (>500000 bp) were only observed in parental cells (Tables S2 and S8). In general, the pattern of lncRNA length distribution

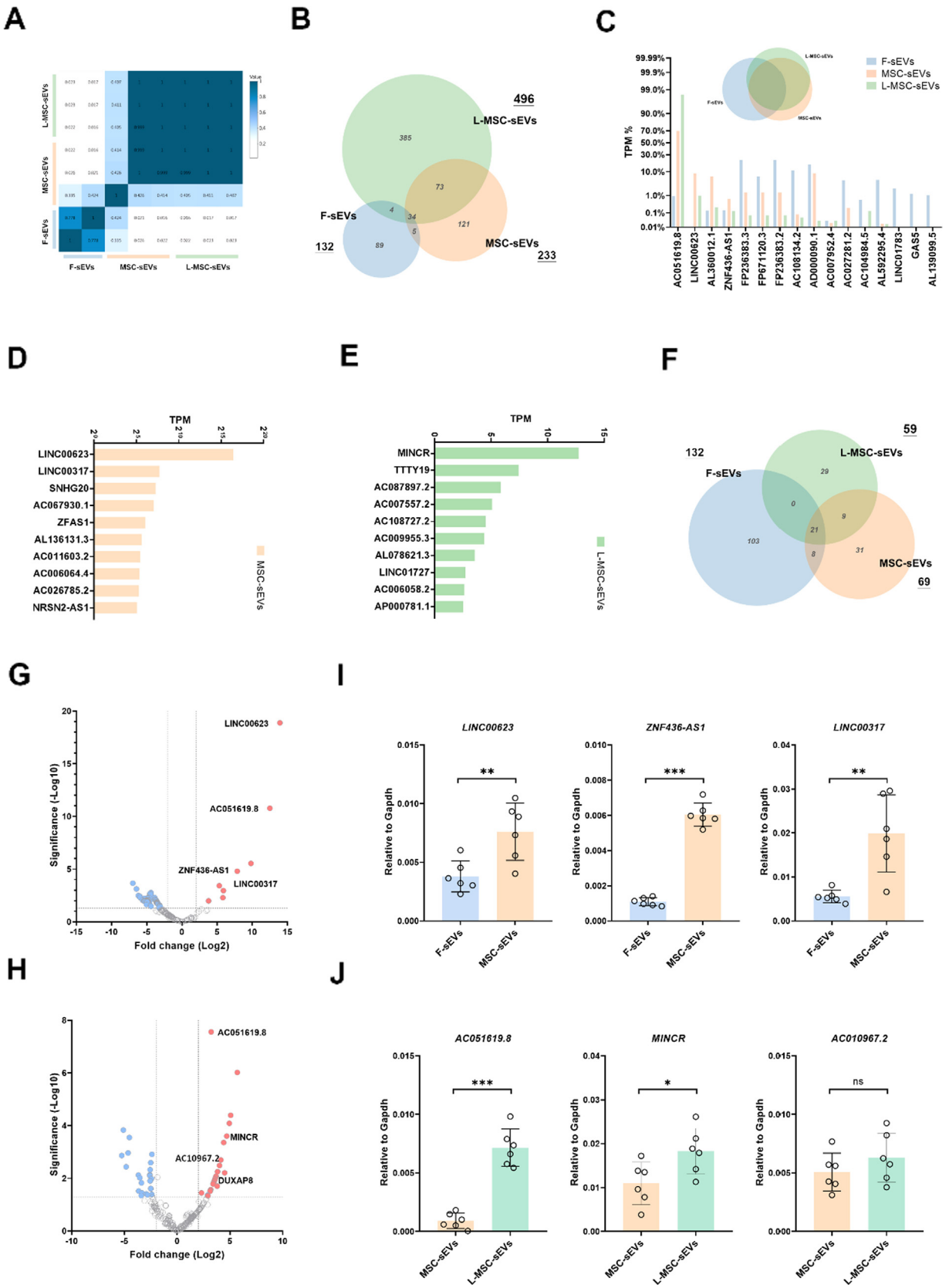
A
L-MSC-sEVs
MSC-sEVs
F-sEVs
F-sEVs
MSC-sEVs
L-MSC-sEVs
B
496
L-MSC-sEVs
385
73
4
34
121
5
89
F-sEVs
132
MSC-sEVs
233
C
F-sEVs
MSC-sEVs
L-MSC-sEVs
TPM %
99.99%
99.9%
99.0%
90.0%
70.0%
50.0%
30.0%
10.0%
1.0%
0.1%
0.01%
AC051619.8
LINC00623
AL360012.1
ZNF436-AS1
FP236383.3
FP671120.3
FP236383.2
AC108134.2
AD000090.1
AC007952.4
AC027281.2
AC104984.5
AL592295.4
LINC01783
GAS5
AL139099.5
D
TPM
LINC00623
LINC00317
SNHG20
AC067930.1
ZFAS1
AL136131.3
AC011603.2
AC006064.4
AC026785.2
NRSN2-AS1
MSC-sEVs
E
TPM
MINCR
TTTY19
AC087897.2
AC007557.2
AC108727.2
AC009955.3
AL078621.3
LINC01727
AC006058.2
AP000781.1
L-MSC-sEVs
F
59
132
L-MSC-sEVs
F-sEVs
29
0
9
21
103
8
31
MSC-sEVs
69
G
Significance (-Log10)
Fold change (Log2)
LINC00623
AC051619.8
ZNF436-AS1
LINC00317
I
LINC00623
ZNF436-AS1
LINC00317
Relative to Gapdh
F-sEVs
MSC-sEVs
H
Significance (-Log10)
Fold change (Log2)
AC051619.8
MINCR
AC10967.2
DUXAP8
J
AC051619.8
MINCR
AC010967.2
Relative to Gapdh
MSC-sEVs
L-MSC-sEVs
ns

Table 1
The top 10 enriched lncRNAs in F-sEVs.

F-sEVs					
lncRNAs	**TPM**	**%**	**Chr**	**Type**	**Length (nt)**
ENSG00000281181.1_FP236383.3	225,476	22.55	chr21	lincRNA	922
ENSG00000280614.1_FP236383.2	225,476	22.55	chr21	lincRNA	922
ENSG00000283907.1_AD000090.1	168,176	16.82	chr19	antisense_RNA	23,998
ENSG00000261889.1_AC108134.2	111,412	11.14	chr16	lincRNA	747
ENSG00000280800.1_FP671120.3	69,167	6.92	chr21	lincRNA	922
ENSG00000283696.1_AL592295.4	50,692	5.07	chr1	lincRNA	23,015
ENSG00000279123.1_AC027281.2	50,151	5.02	chr16	TEC	712
ENSG00000233421.4_LINC01783	21,568	2.16	chr1	lincRNA	2286
ENSG00000234741.7_GAS5	12,164	1.22	chr1	processed_transcript	4982
ENSG00000283029.1_AL139099.5	10,502	1.05	chr14	non_coding	299
Sum	**944,784**	**94.5**	–	–	–

Table 2
The top 10 enriched lncRNAs in MSC-sEVs.

MSC-sEVs					
lncRNAs	**TPM**	**%**	**Chr**	**Type**	**Length (nt)**
ENSG00000260035.1_AC051619.8	695,743	69.57	chr15	sense_intronic	307
ENSG00000283907.1_AD000090.1	89,857	8.99	chr19	antisense_RNA	23,998
ENSG00000226067.6_LINC00623	88,681	8.87	chr1	lincRNA	96,016
ENSG00000270103.3_AL360012.1	67,994	6.8	chr1	lincRNA	130
ENSG00000281181.1_FP236383.3	14,001	1.4	chr21	lincRNA	922
ENSG00000280800.1_FP671120.3	14,001	1.4	chr21	lincRNA	922
ENSG00000280614.1_FP236383.2	14,001	1.4	chr21	lincRNA	922
ENSG00000249087.6_ZNF436-AS1	6612.1	0.66	chr1	antisense_RNA	2842
ENSG00000279123.1_AC027281.2	2149.7	0.21	chr16	TEC	712
ENSG00000266919.3_AC104984.5	1330.8	0.13	chr17	sense_intronic	93
Sum	**994370.6**	**99.43**	**–**	**–**	**–**

Table 3
The top 10 enriched lncRNAs in L-MSC-sEVs.

L-MSC-sEVs					
lncRNAs	**TPM**	**%**	**Chr**	**Type**	**Length (nt)**
ENSG00000260035.1_AC051619.8	982771.16	98.28	chr15	sense_intronic	307
ENSG00000226067.6_LINC00623	9769.68	0.98	chr1	lincRNA	96,016
ENSG00000270103.3_AL360012.1	2196.64	0.22	chr1	lincRNA	130
ENSG00000249087.6_ZNF436-AS1	1338.81	0.13	chr1	antisense_RNA	2842
ENSG00000281181.1_FP236383.3	710.24	0.07	chr21	lincRNA	922
ENSG00000280800.1_FP671120.3	710.24	0.07	chr21	lincRNA	922
ENSG00000280614.1_FP236383.2	710.24	0.07	chr21	lincRNA	922
ENSG00000261889.1_AC108134.2	476.68	0.05	chr16	lincRNA	747
ENSG00000283907.1_AD000090.1	285.4	0.03	chr19	antisense_RNA	23,998
ENSG00000262202.4_AC007952.4	266.98	0.03	chr17	lincRNA	636
Sum	**999236.07**	**99.93**	–	**–**	**–**

between F-sEVs and fibroblasts, as well as between MSC-sEVs and MSCs, was consistent (Fig. 7B, Table S8). Regarding the classification of lncRNAs, antisense RNAs and noncoding RNAs were enriched in both cell types compared with their sEVs; however, lincRNAs and sense intronic RNAs were enriched in both types of sEV types compared with their parental cells (Fig. 7C, Table S9). Similar to the observation for sEVs, most lncRNAs in parental cells were transcribed from chromosomes 1 and 17, but the chromosomal distribution of lncRNAs between sEVs and their parental cells differed (Fig. 7D-E, Table S10).

Fig. 5. Identification of human MSC-sEV-lncRNAs. (A) Distance mapping of lncRNAs using Pearson's correlation coefficient between F-sEVs, MSCs-sEVs and L-MSC-sEVs. (B) Venn diagrams illustrating convergence and noncongruency of lncRNAs. (C) Comparison of the top 10 enriched lncRNAs between F-sEVs, MSCs-sEVs and L-MSC-sEVs. (D) The top 10 newly loaded lncRNAs in MSC-sEVs compared with F-sEVs. (E) The top 10 newly loaded lncRNAs in L-MSC-sEVs compared with MSC-sEVs. (F) Venn diagrams illustrating convergence and noncongruency of lncRNAs. TPM cutoff > 2. (G) Differentially expressed lncRNAs of MSCs-sEVs and F-sEVs revealed by volcano plots. The abscissa corresponds to the fold change (log2); ordinates represent significance (-log10). A log2-fold-change (log2 FC) > 1 and a P value < 0.05 were used to identify differentially expressed lncRNAs. Red dots represent significantly upregulated lncRNAs and blue dots significantly downregulated lncRNAs in MSC-sEVs. (H) Expression levels of DE lncRNAs between MSCs-sEVs and F-sEVs were detected by qRT-PCR (n = 3). (I) Differentially expressed lncRNAs of MSCs-sEVs and L-MSCs-sEVs revealed by volcano plots. The abscissa corresponds to the fold change (log2); ordinates represent significance (-log10). A log2-fold-change (log2 FC) > 1 and a P value < 0.05 were used to identify differentially expressed lncRNAs. Red dots represent significantly upregulated lncRNAs and blue dots significantly downregulated lncRNAs in L-MSC-sEVs. (J) Expression levels of DE lncRNAs between MSCs-sEVs and L-MSCs-sEVs were detected by qRT-PCR (n = 6). Statistical analyses were performed by Student's *t*-test for panels I and J (*P < 0.05, **P < 0.01, *** P < 0.001; ns, not significant).

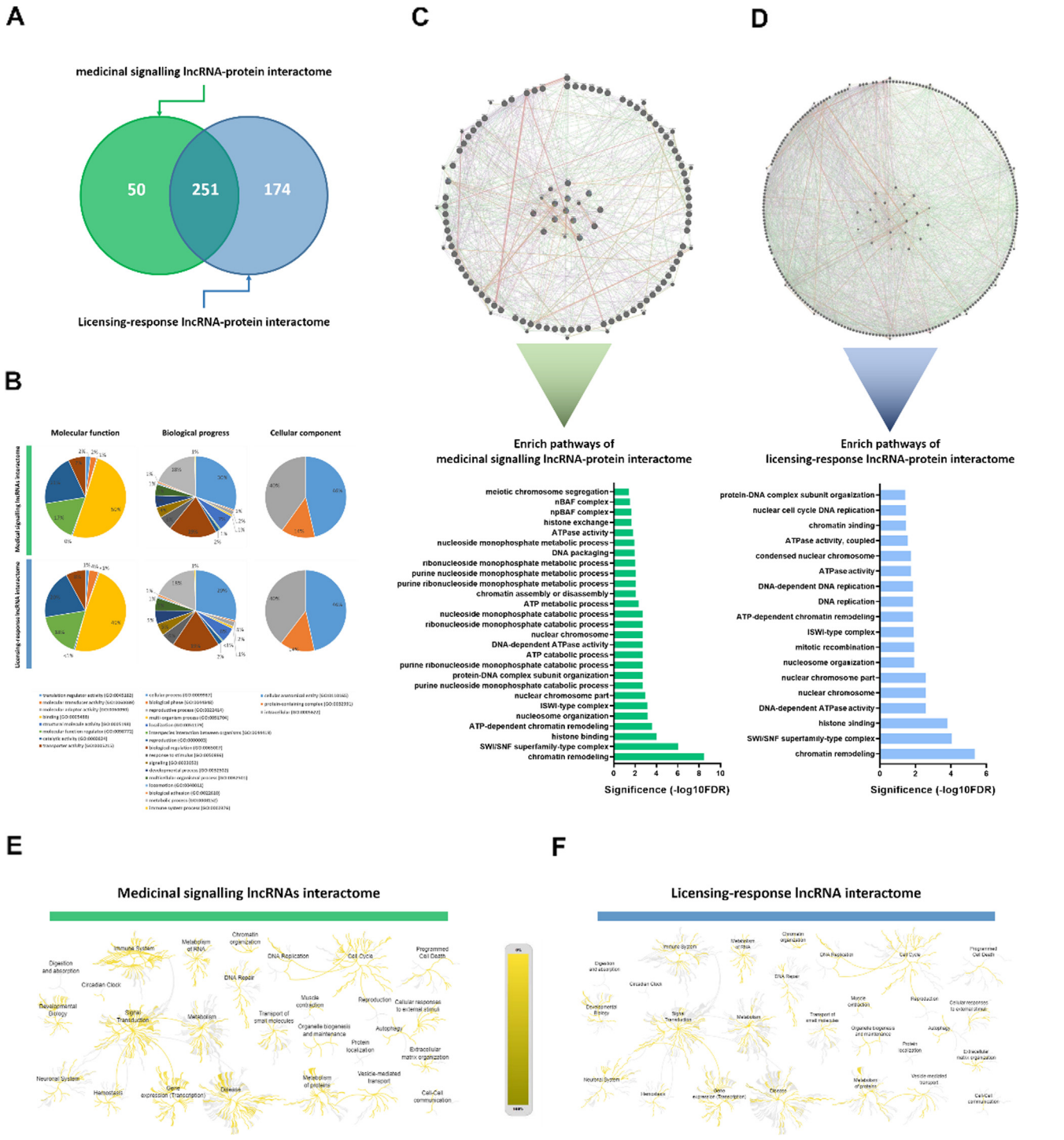

Fig. 6. Characteristics of medicinal signaling lncRNA- and licensing-responsive lncRNA-protein interactomes. (A) Venn diagrams illustrating convergence and noncongruence of predicted interacting proteins of medicinal signaling lncRNAs and licensing-responsive lncRNAs. (B) Functional classifications of the medicinal signaling lncRNA interactome and licensing-responsive lncRNA interactome according to their biological processes, cellular components, and molecular functions. (C-D) Functional enrichment analysis of the medicinal signaling lncRNA interactome (C) and licensing-responsive lncRNA interactome (D) by the Genemania online tool. Purple lines indicate coexpression of proteins, red lines indicate physical interactions between proteins, orange lines represent predicted interactions between proteins, blue lines show colocalization between proteins, and green lines denote genetic interactions. (E-F) Overview of enriched pathways of medicinal signaling lncRNAs interactome (E) and licensing-responsive lncRNA interactome (F) by the Reactome online tool. The yellow key represents the coverage of identified pathways.

Surprisingly, a distinct correlation of lncRNAs in sEVs and parental cells was observed for both fibroblasts (Fig. 7F) and MSCs (Fig. 7G). A total of 2235 lncRNAs were identified in fibroblasts, with only 49 lncRNAs coexisting in F-sEVs (Fig. 7H). A total of 858 lncRNAs were identified in MSCs and fibroblasts, but only 94 coexisted in MSC-sEVs (Fig. 7I). The most enriched lncRNA in MSC-sEVs, AC051619.8, accounted for 69% of all lncRNAs but accounted for only 0.04% of all lncRNAs in MSCs; F-sEV-enriched FP236383.3 and AD000090.1 accounted for 22.5% and 16.8% of all lncRNAs in F-sEVs but only occupied 10.8% and 0.32% of all lncRNAs in fibroblasts, respectively. Differences in lncRNA signatures between parental cells and sEVs were observed for both stem

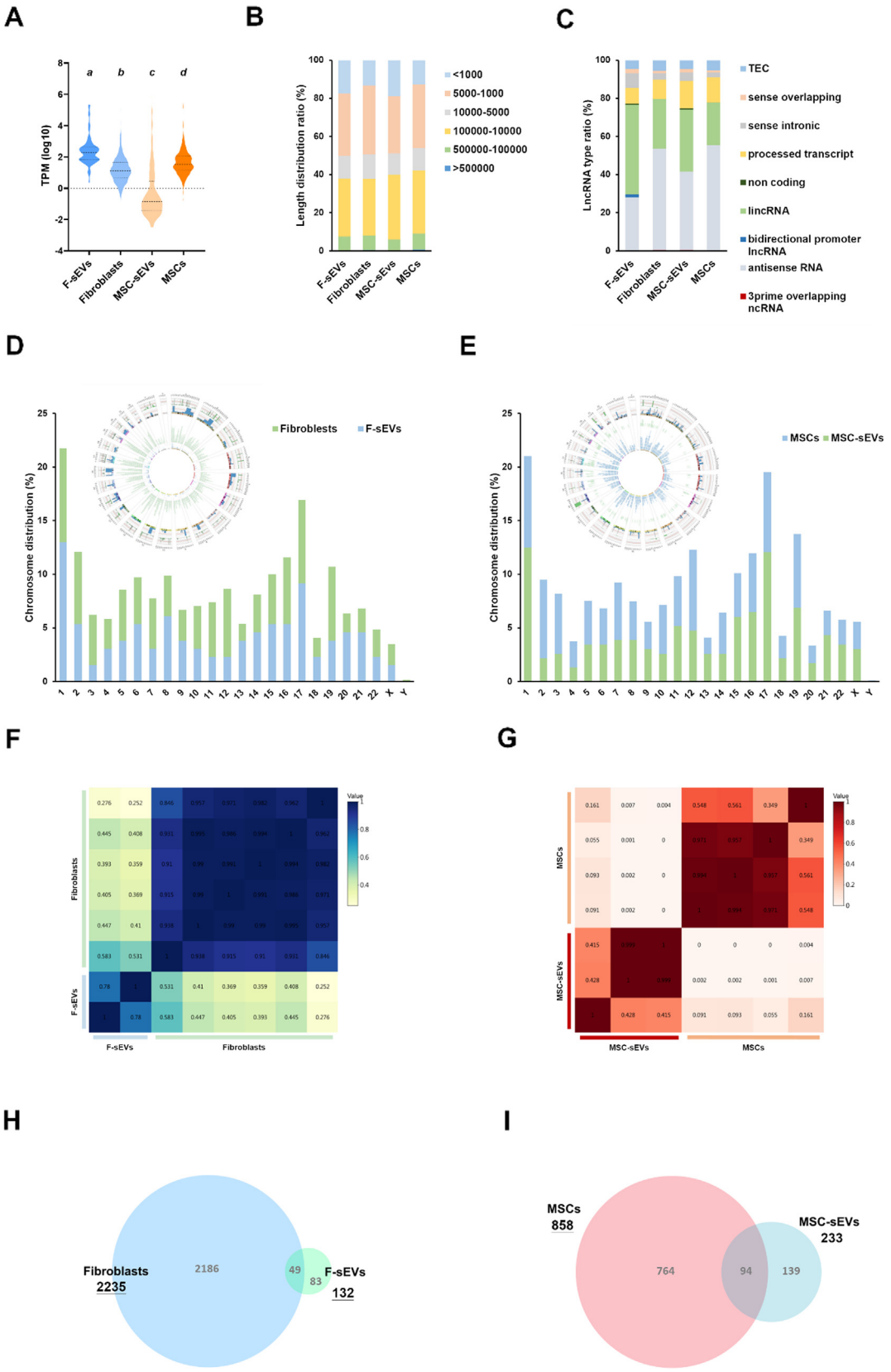

Fig. 7. Comparison of lncRNA characteristics between sEVs and parental cells. (A) The TPM distribution of all identified lncRNAs. (B) Length distribution of lncRNAs. (C) Classification of lncRNAs in sEVs and parental cells into nine categories. (D-E) Chromosomal distribution of lncRNAs in F-sEVs and fibroblasts (D) and MSC-sEVs and MSCs (E). The outer ring represents the lncRNAs labeled with chromosome number and position. A histogram revealed the percentage of chromosome distribution of lncRNAs. (F-G) Pearson's correlation analysis of lncRNAs from F-sEVs and fibroblasts (F) and from MSC-sEVs and MSCs (G). (H-I) Venn diagrams illustrating the convergence and noncongruency of lncRNAs from F-sEVs and fibroblasts (H) and from MSC-sEVs and MSCs (I). TPM cutoff > 0.

cells and fibroblasts, suggesting that rather than a stochastic event, a novel mechanism exists to select the sEV lncRNA cargo The selective lncRNA packaging mechanism shapes the unique lncRNA profile in sEVs and plays a vital role in cell–cell communication under physiological and pathological conditions.

Discussion

Undisputedly, MSC-sEVs create a new therapeutic paradigm for regenerative medicine due to their preponderance over MSC transplantation [55]. MSC-sEVs possess stability, strong biocompatibility, and high therapeutic expandability via various modifications of parental cells. Moreover, compared with parental cells, transplantation of MSC-sEVs has lower risks of immunogenicity, genomic alterations, senescence-induced genetic instability, and pulmonary embolism [56,57]. Clinical trials of MSC-sEVs demonstrate their increased application as a presumptive surrogate to MSC-based therapeutics, yet without an understanding of their intricate properties and how their therapeutic effects are mediated. Indeed, a lack of a deep understanding of the intrinsic composition of MSC-sEVs under physiological and pathological conditions will restrict their clinical applications. Herein, we provide an atlas of lncRNAs in MSC-sEVs with the goal of identifying medicinal signaling lncRNAs using a bioinformatics approach. We further robustly characterized MSC-sEVs under inflammatory cytokine stimulation, which partly mimics the niche of transplanted MSCs under various pathophysiological conditions. The core findings were that MSC-sEVs have a unique lncRNA atlas and that the yield and intrinsic properties of MSC-sEVs are sensitive to inflammatory stimulation, which might correlate with their therapeutic potential *in vivo*. To the best of our knowledge, this is the first study to elucidate and annotate lncRNAs in human MSC-sEVs with or without inflammatory cytokine stimulation. By identifying medicinal signaling lncRNAs, future studies may investigate the therapeutic potential of medicinal signaling lncRNAs under various disease conditions.

LncRNAs appear to participate in many processes, such as RNA splicing, transcription, RNA localization, RNA decay, translation, and epigenetic remodeling, through their unique sequence and structure [54], and the topological structures of DNA controlled by cohesion, CTCF, histone and chromatin-associated protein complexes are dominant in the generation of gene regulatory networks. By connecting those nuclear elements, lncRNAs alter the three-dimensional organization of DNA to regulate transcription [58]. Functional enrichment analysis revealed medicinal signaling lncRNA-interacting proteins to be enriched in nuclear activity such as ATP-dependent chromatin remodeling, SWI/SNF complex and nBAF, which is implicated in development and neuron disorders [59]. Although sublocalization of MSC-sEV lncRNAs in recipient cells requires further investigation, our results suggest that MSC-sEVs regulate transcriptional activity in recipient cells by affecting higher-order chromatin structures.

Growing evidence reveals that lncRNAs in MSC-sEVs mediate the biological functions of these vesicles [18–20,60]. By RNA sequencing and robust computational pipeline analysis, we identified a cluster of medicinal signaling lncRNA, which lncRNAs that are specific to and enriched in MSC-sEVs but not F-sEVs. For instance, LINC00623, the most abundant newly loaded lncRNA in MSC-sEVs, is increasingly downregulated with osteoarthritis severity, which causes chondrocyte apoptosis and extracellular matrix degradation [50]. As LINC00623 is specific and enriched in MSC-sEVs, it might act as a dominant medicinal signaling lncRNA of MSC-sEVs in osteoarthritis treatment [61,62]. Based on our *in silico* prediction, the LINC00623-interacting proteins PIK3R4, CHMP7, ROCK1 and ARID4B are associated with SARS-CoV-1/2 infection. Furthermore, ROCK1 and ARID4B (HDAC complex) are associated with therapeutics for SARS/COVID-19 [63–65]. Indeed, inhibition of HDAC in COVID-19 treatment seems to occur by reducing ACE2, a receptor for SARS-CoV-1/2 entry into cells [63,66].

Unlike proteins and miRNAs, expression of lncRNAs is not conserved across species [67,68], indicating that lncRNA expression in the same cell type varies among species. Therefore, it is paramount to verify lncRNAs in human sEVs prior to further mechanistic interpretation and clinical application. Recently, it has been reported that by delivering lncRNA H19, sEVs from rodent MSCs possess therapeutic potential in wound healing and myocardial infarction [18,20]. Exosomal lncRNA H19 from mouse MSCs accelerate wound healing via regulation of miR-152-3p-mediated PTEN inhibition, and rat MSC-exosomal lncRNA H19 protects cardiomyocytes against apoptosis via regulation of miR-675 in endothelial cells. Surprisingly, lncRNA H19 was hardly detected in human MSC-sEVs in our study: it was identified in only one MSC-sEV sample among six samples, with a low expression level of approximately 0.05 TPM, and seems unlikely to have dramatic biological effects compared to other abundant lncRNAs. Regardless, the possibility of the butterfly effect on transcriptomic or epigenomic regulation in recipient cells by rarely expressed lncRNAs in sEVs should not be excluded.

Although numerous studies have proven the efficacy of MSCs for treating inflammatory-related diseases [69], the curative effect is not consistent. For instance, the therapeutic effectiveness of MSCs on graft-versus-host disease ranges from 15 to 94% in clinical trials [70–74], which might be attributed to divergent changes in the MSC *in vivo* microenvironment. Indeed, previous reports have shown that inflammatory cytokines shape protein and miRNA patterns to boost the therapeutic ability of MSC-sEVs [32,75]. Herein, we demonstrate that the lncRNA landscape also responds to inflammatory cytokines. Inflammatory stimulation upregulated lncRNA MINCR and DUXAP8 in MSC-sEVs. However, MINCR and DUXAP8 are implicated in tumor progression [51,52,76,77] through Wnt/β-catenin pathway activation, a crucial signaling pathway also involved in tissue regeneration [78,79]. Some identified lncRNAs in L-MSC-sEVs are related to tumor development, which might be attributed to most investigations on lncRNAs being in cancer studies. Indeed, there is still limited literature regarding the role of MSC-sEV lncRNAs, and whether inflammatory stimulation boosts or blunts the therapeutic efficacy of MSC-sEVs via lncRNA reprogramming remains unclear. Our study provides groundwork for future investigations on MSC-sEV lncRNAs regarding regenerative medicine and even tumorigenesis in pathological conditions. Further experimental characterization to identify the accurate roles and therapeutic candidates of medicinal signaling lncRNAs is critical for developing a lncRNA-based intervention.

Compared to protein-coding transcripts, cellular lncRNAs are relatively lineage- and tissue-specific in a spatiotemporal manner [80–83]. Despite the fact that tissue specificity is observed for sEV-lncRNAs, the patterns are distinct from their parental cells. Similar to previous findings in cancer-associated fibroblasts and their derived exosomes [84], distinct lncRNA profiles between parental cells and sEVs were also observed for both MSCs and fibroblasts, indicating a novel lineage-specific mechanism to selectively sort lncRNAs toward sEVs rather than merely lineage specificity of the cellular lncRNAs itself. On the other hand, the encapsulation of exogenous therapeutic materials and genetic modification of parental cells to boost the therapeutic ability of sEVs are new therapeutic avenues. Further investigation into the selective packaging mechanism will enhance packaging efficiency and provide better therapeutic opportunities for patients.

Minimal criteria for defining MSCs, including morphology, surface markers, and multipotency, were established by the International Society for Cell and Gene Therapy in 2006 [35], but those characteristics do not reflect the clinical therapeutic efficacy and

mechanism of action of MSCs. On the other hand, the characteristics of EVs were defined in the Minimal Information for Studies of EVs (MISEV2014) in 2014 [85] and renewed to MISEV2018 [37] by the International Society for Extracellular Vesicles (ISEV). Although the key definition of physical and biological characteristics of MSC-sEVs has been discussed [38], the current criteria do not provide guidance on functional testing of the biological activities of MSC-sEVs, which relies on distinct components inside the vesicles, which are distinguishable from non-MSC-sEVs, i.e., F-sEVs. Overall, the therapeutic ability of MSC-sEVs hinges on the synergistic effects of their intricate contents targeting different therapeutic pathways in recipient cells rather than only a few key molecules. In this study, we elucidated the lncRNA landscapes in MSC-sEVs and F-sEVs. Furthermore, we improved the systematic understanding of component diversity within MSC-sEVs under inflammatory conditions, which will provide certain advantages for defining the characteristics and therapeutic indications of MSC-sEVs as quantifiable features.

The present *in silico* study still has some limitations. The protein and miRNA profiles of MSC-sEVs are distinct in MSCs harvested from different origins and cultured under different conditions that impact the biological effects and therapeutic capacity of MSC-sEVs [86–88]. We analyzed sEVs derived from human male adipose-derived MSCs, and it remains unclear whether origin or sex affects the lncRNA landscape in sEVs in response to inflammation. Some of the RNA sequencing data obtained from public repositories and the different sample preparation and library construction processes may introduce bias; enlarging the sample size and standardizing sample operations will reduce differences between experimental conditions in future investigations. Because a comprehensive functional annotation of lncRNAs is lacking, we predicted lncRNA function by an *in silico* approach, which may overlook lncRNA functions in nature, particularly effects at the posttranscriptional level. Additionally, the functional roles of identified medicinal signaling lncRNAs in MSC-sEVs require further investigation *in vivo*.

Conclusion

This study provides valuable information regarding the lncRNA landscapes of sEVs derived from human naïve MSCs and licensed MSCs. Understanding the fingerprint of lncRNAs in MSC-sEVs will provide a new avenue for defining a standard of therapeutic sEVs and developing efficacious precision-engineered MSC-sEVs [89–91]. Using next-generation CRISPR-Cas technologies and preloading with specific therapeutic molecules, i.e., medicinal signaling lncRNAs, may provide a new perspective therapeutic regimen in precision nanomedicine.

Compliance with ethics requirements

No human or animal subjects are involved in this article.

CRediT authorship contribution statement

Chien-Wei Lee: Conceptualization, Methodology, Writing – original draft, Funding acquisition. **Yi-Fan Chen:** Writing – original draft, Writing – review & editing. **Allen Wei-Ting Hsiao:** Investigation, Validation. **Amanda Yu-Fan Wang:** Formal analysis, Methodology. **Oscar Yuan-Jie Shen:** Writing – review & editing. **Belle Yu-Hsuan Wang:** Investigation, Validation. **Lok Wai Cola Ho:** Investigation. **Wei-Ting Lin:** Investigation, Validation. **Chung Hang Jonathan Choi:** Resources. **Oscar Kuang-Sheng Lee:** Writing – review & editing, Supervision, Writing – review & editing, Project administration.

Declaration of Competing Interest

The authors declare that they have no known competing financial interests or personal relationships that could have appeared to influence the work reported in this paper.

Acknowledgements

This work was supported by the Hong Kong Government Research Grant Council, General Research Fund (Reference no. 14104620) to CW Lee and by China Medical University Hospital (Reference no. DMR-110-226) to OK Lee. The authors also thank Prof. HH Cheung at the School of Biomedical Sciences, Faculty of Medicine, The Chinese University of Hong Kong, Hong Kong for the generous gift of human skin fibroblasts (GM08429). Fig. 1 is created with materials from BioRender.com.

Appendix A. Supplementary material

Supplementary data to this article can be found online at https://doi.org/10.1016/j.jare.2021.11.003.

References

[1] Caplan AI. Mesenchymal Stem Cells: Time to Change the Name! Stem Cells Transl Med 2017;6(6):1445–51. doi: https://doi.org/10.1002/sctm.17-0051.
[2] Galipeau J. Mesenchymal Stromal Cells for Graft-versus-Host Disease: A Trilogy. Biol Blood Marrow Transplant 2020;26(5):e89–91. doi: https://doi.org/10.1016/j.bbmt.2020.02.023.
[3] Lee CW, Chen YF, Wu HH, Lee OK. Historical Perspectives and Advances in Mesenchymal Stem Cell Research for the Treatment of Liver Diseases. Gastroenterology 2018;154(1):46–56. doi: https://doi.org/10.1053/j.gastro.2017.09.049.
[4] Yin JQ, Zhu J, Ankrum JA. Manufacturing of primed mesenchymal stromal cells for therapy. Nat Biomed Eng 2019;3(2):90–104. doi: https://doi.org/10.1038/s41551-018-0325-8.
[5] Hu C-H, Tseng Y-W, Lee C-W, Chiou C-Y, Chuang S-S, Yang J-Y, et al. Combination of mesenchymal stem cell-conditioned medium and botulinum toxin type A for treating human hypertrophic scars. J Plast Reconstr Aesthet Surg 2020;73(3):516–27. doi: https://doi.org/10.1016/j.bjps.2019.07.010.
[6] Xu H, Lee C-W, Wang Y-F, Huang S, Shin L-Y, Wang Y-H, et al. The Role of Paracrine Regulation of Mesenchymal Stem Cells in the Crosstalk With Macrophages in Musculoskeletal Diseases: A Systematic Review. Front Bioeng Biotechnol 2020;8. doi: https://doi.org/10.3389/fbioe.2020.587052.
[7] Bateman ME, Strong AL, Gimble JM, Bunnell BA. Concise Review: Using Fat to Fight Disease: A Systematic Review of Nonhomologous Adipose-Derived Stromal/Stem Cell Therapies. Stem Cells 2018;36(9):1311–28. doi: https://doi.org/10.1002/stem.2847.
[8] Mendt M, Rezvani K, Shpall E. Mesenchymal stem cell-derived exosomes for clinical use. Bone Marrow Transplant 2019;54(Suppl 2):789–92. doi: https://doi.org/10.1038/s41409-019-0616-z.
[9] Lee C-W, Hsiao W-T, Lee O-S. Mesenchymal stromal cell-based therapies reduce obesity and metabolic syndromes induced by a high-fat diet. Transl Res 2017;182:61–74.e8. doi: https://doi.org/10.1016/j.trsl.2016.11.003.
[10] Elahi FM, Farwell DG, Nolta JA, Anderson JD. Preclinical translation of exosomes derived from mesenchymal stem/stromal cells. Stem Cells 2020;38(1):15–21. doi: https://doi.org/10.1002/stem.3061.
[11] van Niel G, D'Angelo G, Raposo G. Shedding light on the cell biology of extracellular vesicles. Nat Rev Mol Cell Biol 2018;19(4):213–28. doi: https://doi.org/10.1038/nrm.2017.125.
[12] Raposo G, Stoorvogel W. Extracellular vesicles: exosomes, microvesicles, and friends. J Cell Biol 2013;200(4):373–83. doi: https://doi.org/10.1083/jcb.201211138.
[13] Thakur BK, Zhang H, Becker A, Matei I, Huang Y, Costa-Silva B, et al. Double-stranded DNA in exosomes: a novel biomarker in cancer detection. Cell Res. 2014;24(6):766–9. doi: https://doi.org/10.1038/cr.2014.44.
[14] Sato-Kuwabara Y, Melo SA, Soares FA, Calin GA. The fusion of two worlds: non-coding RNAs and extracellular vesicles–diagnostic and therapeutic implications (Review). Int J Oncol 2015;46(1):17–27. doi: https://doi.org/10.3892/ijo.2014.2712.
[15] Baglio SR, Rooijers K, Koppers-Lalic D, Verweij FJ, Pérez Lanzón M, Zini N, et al. Human bone marrow- and adipose-mesenchymal stem cells secrete exosomes enriched in distinctive miRNA and tRNA species. Stem Cell Res Ther 2015;6(1). doi: https://doi.org/10.1186/s13287-015-0116-z.
[16] Skotland T, Sandvig K, Llorente A. Lipids in exosomes: Current knowledge and the way forward. Prog Lipid Res 2017;66:30–41. doi: https://doi.org/10.1016/j.plipres.2017.03.001.

[17] Kazimierczyk M, Kasprowicz MK, Kasprzyk ME, Wrzesinski J. Human Long Noncoding RNA Interactome: Detection, Characterization and Function. Int J Mol Sci 2020;21(3). doi: https://doi.org/10.3390/ijms21031027.
[18] Li Bo, Luan S, Chen J, Zhou Y, Wang T, Li Z, et al. The MSC-Derived Exosomal lncRNA H19 Promotes Wound Healing in Diabetic Foot Ulcers by Upregulating PTEN via MicroRNA-152-3p. Mol Ther Nucleic Acids 2020;19:814–26. doi: https://doi.org/10.1016/j.omtn.2019.11.034.
[19] Liu Y, Zou R, Wang Z, Wen C, Zhang F, Lin F. Exosomal KLF3-AS1 from hMSCs promoted cartilage repair and chondrocyte proliferation in osteoarthritis. Biochem J 2018;475(22):3629–38. doi: https://doi.org/10.1042/BCJ20180675.
[20] Huang P, Wang L, Li Q, Tian X, Xu J, Xu J, et al. Atorvastatin enhances the therapeutic efficacy of mesenchymal stem cells-derived exosomes in acute myocardial infarction via up-regulating long non-coding RNA H19. Cardiovasc Res 2020;116(2):353–67. doi: https://doi.org/10.1093/cvr/cvz139.
[21] Bernardo ME, Fibbe WE. Mesenchymal stromal cells: sensors and switchers of inflammation. Cell Stem Cell 2013;13(4):392–402. doi: https://doi.org/10.1016/j.stem.2013.09.006.
[22] Okada S, Ogata T. Inflammation and regeneration in cross-organs. Inflamm Regen 2016;36:18. doi: https://doi.org/10.1186/s41232-016-0023-4.
[23] Forbes SJ, Rosenthal N. Preparing the ground for tissue regeneration: from mechanism to therapy. Nat Med 2014;20(8):857–69. doi: https://doi.org/10.1038/nm.3653.
[24] Anderson JD, Johansson HJ, Graham CS, Vesterlund M, Pham MT, Bramlett CS, et al. Comprehensive Proteomic Analysis of Mesenchymal Stem Cell Exosomes Reveals Modulation of Angiogenesis via Nuclear Factor-KappaB Signaling. Stem Cells 2016;34(3):601–13. doi: https://doi.org/10.1002/stem.2298.
[25] Showalter MR, Wancewicz B, Fiehn O, Archard JA, Clayton S, Wagner J, et al. Primed mesenchymal stem cells package exosomes with metabolites associated with immunomodulation. Biochem Biophys Res Commun 2019;512(4):729–35. doi: https://doi.org/10.1016/j.bbrc.2019.03.119.
[26] Liang YC, Wu YP, Li XD, Chen SH, Ye XJ, Xue XY, et al. TNF-alpha-induced exosomal miR-146a mediates mesenchymal stem cell-dependent suppression of urethral stricture. J Cell Physiol 2019;234(12):23243–55. doi: https://doi.org/10.1002/jcp.28891.
[27] Mead B, Chamling X, Zack DJ, Ahmed Z, Tomarev S. TNFalpha-Mediated Priming of Mesenchymal Stem Cells Enhances Their Neuroprotective Effect on Retinal Ganglion Cells. Invest Ophthalmol Vis Sci 2020;61(2):6. doi: https://doi.org/10.1167/iovs.61.2.6.
[28] Zhang Q, Fu L, Liang Y, Guo Z, Wang L, Ma C, et al. Exosomes originating from MSCs stimulated with TGF-beta and IFN-gamma promote Treg differentiation. J Cell Physiol 2018;233(9):6832–40. doi: https://doi.org/10.1002/jcp.26436.
[29] Riazifar M, Mohammadi MR, Pone EJ, Yeri A, Lässer C, Segaliny AI, et al. Stem Cell-Derived Exosomes as Nanotherapeutics for Autoimmune and Neurodegenerative Disorders. ACS Nano 2019;13(6):6670–88. doi: https://doi.org/10.1021/acsnano.9b01004.
[30] Huang C, Luo W-F, Ye Y-F, Lin Li, Wang Z, Luo M-H, et al. Characterization of inflammatory factor-induced changes in mesenchymal stem cell exosomes and sequencing analysis of exosomal microRNAs. World J Stem Cells 2019;11(10):859–90. doi: https://doi.org/10.4252/wjsc.v11.i10.859.
[31] Ferguson SW, Wang J, Lee CJ, Liu M, Neelamegham S, Canty JM, et al. The microRNA regulatory landscape of MSC-derived exosomes: a systems view. Sci Rep 2018;8(1):1419. doi: https://doi.org/10.1038/s41598-018-19581-x.
[32] Domenis R, Cifù A, Quaglia S, Pistis C, Moretti M, Vicario A, et al. Pro inflammatory stimuli enhance the immunosuppressive functions of adipose mesenchymal stem cells-derived exosomes. Sci Rep 2018;8(1). doi: https://doi.org/10.1038/s41598-018-31707-9.
[33] Zhu Z, Zhang Y, Wu L, Hua K, Ding J. Regeneration-Related Functional Cargoes in Mesenchymal Stem Cell-Derived Small Extracellular Vesicles. Stem Cells Dev 2020;29(1):15–24. doi: https://doi.org/10.1089/scd.2019.0131.
[34] Marinaro F, Gómez-Serrano M, Jorge I, Silla-Castro JC, Vázquez J, Sánchez-Margallo FM, et al. Unraveling the Molecular Signature of Extracellular Vesicles From Endometrial-Derived Mesenchymal Stem Cells: Potential Modulatory Effects and Therapeutic Applications. Front Bioeng Biotechnol 2019;7. doi: https://doi.org/10.3389/fbioe.2019.00431.
[35] Dominici M, Le Blanc K, Mueller I, Slaper-Cortenbach I, Marini FC, Krause DS, et al. Minimal criteria for defining multipotent mesenchymal stromal cells. The International Society for Cellular Therapy position statement. Cytotherapy 2006;8(4):315–7. doi: https://doi.org/10.1080/14653240600855905.
[36] Lee CW, Huang WC, Huang HD, Huang YH, Ho JH, Yang MH, et al. DNA Methyltransferases Modulate Hepatogenic Lineage Plasticity of Mesenchymal Stromal Cells. Stem Cell Rep 2017;9(1):247–63. doi: https://doi.org/10.1016/j.stemcr.2017.05.008.
[37] Théry C, Witwer KW, Aikawa E, Alcaraz MJ, Anderson JD, Andriantsitohaina R, et al. Minimal information for studies of extracellular vesicles 2018 (MISEV2018): a position statement of the International Society for Extracellular Vesicles and update of the MISEV2014 guidelines. J Extracell Vesicles 2018;7(1):1535750. doi: https://doi.org/10.1080/20013078.2018.1535750.
[38] Witwer KW, Van Balkom BWM, Bruno S, Choo A, Dominici M, Gimona M, et al. Defining mesenchymal stromal cell (MSC)-derived small extracellular vesicles for therapeutic applications. J Extracell Vesicles 2019;8(1):1609206. doi: https://doi.org/10.1080/20013078.2019.1609206.
[39] Frankish A, Diekhans M, Ferreira AM, Johnson R, Jungreis I, Loveland J, et al. GENCODE reference annotation for the human and mouse genomes. Nucleic Acids Res 2019;47(D1):D766–73. doi: https://doi.org/10.1093/nar/gky955.
[40] Ritchie ME, Phipson B, Wu D, Hu Y, Law CW, Shi W, et al. Limma powers differential expression analyses for RNA-sequencing and microarray studies. Nucleic Acids Res 2015;43(7). doi: https://doi.org/10.1093/nar/gkv007.
[41] Lang B, Armaos A, Tartaglia GG. RNAct: Protein-RNA interaction predictions for model organisms with supporting experimental data. Nucleic Acids Res 2019;47(D1):D601–6. doi: https://doi.org/10.1093/nar/gky967.
[42] Jassal B, Matthews L, Viteri G, Gong C, Lorente P, Fabregat A, et al. The reactome pathway knowledgebase. Nucleic Acids Res 2020;48(D1):D498–503. doi: https://doi.org/10.1093/nar/gkz1031.
[43] Mi H, Ebert D, Muruganujan A, Mills C, Albou LP, Mushayamaha T, et al. PANTHER version 16: a revised family classification, tree-based classification tool, enhancer regions and extensive API. Nucleic Acids Res 2020. doi: https://doi.org/10.1093/nar/gkaa1106.
[44] Franz M, Rodriguez H, Lopes C, Zuberi K, Montojo J, Bader GD, et al. GeneMANIA update 2018. Nucleic Acids Res 2018;46(W1):W60–4. doi: https://doi.org/10.1093/nar/gky311.
[45] Au Yeung CL, Co N-N, Tsuruga T, Yeung T-L, Kwan S-Y, Leung CS, et al. Exosomal transfer of stroma-derived miR21 confers paclitaxel resistance in ovarian cancer cells through targeting APAF1. Nat Commun 2016;7(1). doi: https://doi.org/10.1038/ncomms11150.
[46] Jääger K, Islam S, Zajac P, Linnarsson S, Neuman T, Wagner W. RNA-seq analysis reveals different dynamics of differentiation of human dermis- and adipose-derived stromal stem cells. PLoS ONE 2012;7(6):e38833. doi: https://doi.org/10.1371/journal.pone.0038833.
[47] Andreu Z, Yanez-Mo M. Tetraspanins in extracellular vesicle formation and function. Front Immunol 2014;5:442. doi: https://doi.org/10.3389/fimmu.2014.00442.
[48] Kalluri R, LeBleu VS. The biology, function, and biomedical applications of exosomes. Science 2020;367(6478). doi: https://doi.org/10.1126/science.aau6977.
[49] Ma L, Bajic VB, Zhang Z. On the classification of long non-coding RNAs. RNA Biol 2013;10(6):925–33. doi: https://doi.org/10.4161/rna.24604.
[50] Lu G, Li L, Wang B, Kuang L. LINC00623/miR-101/HRAS axis modulates IL-1beta-mediated ECM degradation, apoptosis and senescence of osteoarthritis chondrocytes. Aging (Albany NY) 2020;12(4):3218–37. doi: https://doi.org/10.18632/aging.102801.
[51] Yu Y, Chang Z, Han C, Zhuang L, Zhou C, Qi X, et al. Long non-coding RNA MINCR aggravates colon cancer via regulating miR-708-5p-mediated Wnt/beta-catenin pathway. Biomed Pharmacother 2020;129:. doi: https://doi.org/10.1016/j.biopha.2020.110292110292.
[52] Li H, Yuan R, Wang H, Li C, Wei J. LncRNA MINCR promotes the development of liver cancer by regulating microRNA-107/beta-catenin. J BUON 2020;25(2):972–80.
[53] Li Z, Xie X, Fan X, Li X. Long Non-coding RNA MINCR Regulates miR-876-5p/GSPT1 Axis to Aggravate Glioma Progression. Neurochem Res 2020;45(7):1690–9. doi: https://doi.org/10.1007/s11064-020-03029-8.
[54] Gil N, Ulitsky I. Regulation of gene expression by cis-acting long non-coding RNAs. Nat Rev Genet 2020;21(2):102–17. doi: https://doi.org/10.1038/s41576-019-0184-5.
[55] Rani S, Ryan AE, Griffin MD, Ritter T. Mesenchymal Stem Cell-derived Extracellular Vesicles: Toward Cell-free Therapeutic Applications. Mol Ther 2015;23(5):812–23. doi: https://doi.org/10.1038/mt.2015.44.
[56] Sun Li, Xu R, Sun X, Duan Y, Han Y, Zhao Y, et al. Safety evaluation of exosomes derived from human umbilical cord mesenchymal stromal cell. Cytotherapy 2016;18(3):413–22. doi: https://doi.org/10.1016/j.jcyt.2015.11.018.
[57] Ela S, Mager I, Breakefield XO, Wood MJ. Extracellular vesicles: biology and emerging therapeutic opportunities. Nat Rev Drug Discov 2013;12(5):347–57. doi: https://doi.org/10.1038/nrd3978.
[58] Maass PG, Barutcu AR, Rinn JL. Interchromosomal interactions: A genomic love story of kissing chromosomes. J Cell Biol 2019;218(1):27–38. doi: https://doi.org/10.1083/jcb.201806052.
[59] Alfert A, Moreno N, Kerl K. The BAF complex in development and disease. Epigenetics Chromatin 2019;12(1):19. doi: https://doi.org/10.1186/s13072-019-0264-y.
[60] Deng M, Yuan H, Liu S, Hu Z, Xiao H. Exosome-transmitted LINC00461 promotes multiple myeloma cell proliferation and suppresses apoptosis by modulating microRNA/BCL-2 expression. Cytotherapy 2019;21(1):96–106. doi: https://doi.org/10.1016/j.jcyt.2018.10.006.
[61] Mianehsaz E, Mirzaei HR, Mahjoubin-Tehran M, Rezaee A, Sahebnasagh R, Pourhanifeh MH, et al. Mesenchymal stem cell-derived exosomes: a new therapeutic approach to osteoarthritis? Stem Cell Res Ther 2019;10(1). doi: https://doi.org/10.1186/s13287-019-1445-0.
[62] Lee Y-H, Park H-K, Auh Q-S, Nah H, Lee JS, Moon H-J, et al. Emerging Potential of Exosomes in Regenerative Medicine for Temporomandibular Joint Osteoarthritis. Int J Mol Sci 2020;21(4):1541. doi: https://doi.org/10.3390/ijms21041541.
[63] Teodori L, Sestili P, Madiai V, Coppari S, Fraternale D, Rocchi MBL, et al. MicroRNAs Bioinformatics Analyses Identifying HDAC Pathway as a Putative Target for Existing Anti-COVID-19 Therapeutics. Front Pharmacol 2020;11. doi: https://doi.org/10.3389/fphar.2020.582003.
[64] Mousavi SZ, Rahmanian M, Sami A. A connectivity map-based drug repurposing study and integrative analysis of transcriptomic profiling of SARS-CoV-2 infection. Infect Genet Evol 2020;86:104610. doi: https://doi.org/10.1016/j.meegid.2020.104610.

[65] Bouhaddou M, Memon D, Meyer B, White KM, Rezelj VV, Correa Marrero M, et al. The Global Phosphorylation Landscape of SARS-CoV-2 Infection. Cell 2020;182(3):685–712.e19. doi: https://doi.org/10.1016/j.cell.2020.06.034.
[66] Takahashi Y, Hayakawa A, Sano R, Fukuda H, Harada M, Kubo R, et al. Histone deacetylase inhibitors suppress ACE2 and ABO simultaneously, suggesting a preventive potential against COVID-19. Sci Rep 2021;11(1). doi: https://doi.org/10.1038/s41598-021-82970-2.
[67] Lagos-Quintana M, Rauhut R, Lendeckel W, Tuschl T. Identification of novel genes coding for small expressed RNAs. Science 2001;294(5543):853–8. doi: https://doi.org/10.1126/science.1064921.
[68] Meunier J, Lemoine F, Soumillon M, Liechti A, Weier M, Guschanski K, et al. Birth and expression evolution of mammalian microRNA genes. Genome Res 2013;23(1):34–45. doi: https://doi.org/10.1101/gr.140269.112.
[69] Harrell CR, Jovicic N, Djonov V, Arsenijevic N, Volarevic V. Mesenchymal Stem Cell-Derived Exosomes and Other Extracellular Vesicles as New Remedies in the Therapy of Inflammatory Diseases. Cells 2019;8(12):1605. doi: https://doi.org/10.3390/cells8121605.
[70] Le Blanc K, Rasmusson I, Sundberg B, Götherström C, Hassan M, Uzunel M, et al. Treatment of severe acute graft-versus-host disease with third party haploidentical mesenchymal stem cells. Lancet 2004;363(9419):1439–41. doi: https://doi.org/10.1016/S0140-6736(04)16104-7.
[71] Le Blanc K, Frassoni F, Ball L, Locatelli F, Roelofs H, Lewis I, et al. Mesenchymal stem cells for treatment of steroid-resistant, severe, acute graft-versus-host disease: a phase II study. Lancet 2008;371(9624):1579–86. doi: https://doi.org/10.1016/S0140-6736(08)60690-X.
[72] Kebriaei P, Isola L, Bahceci E, Holland K, Rowley S, McGuirk J, et al. Adult human mesenchymal stem cells added to corticosteroid therapy for the treatment of acute graft-versus-host disease. Biol Blood Marrow Transplant 2009;15(7):804–11. doi: https://doi.org/10.1016/j.bbmt.2008.03.012.
[73] von Bonin M, Stölzel F, Goedecke A, Richter K, Wuschek N, Hölig K, et al. Treatment of refractory acute GVHD with third-party MSC expanded in platelet lysate-containing medium. Bone Marrow Transplant 2009;43(3):245–51. doi: https://doi.org/10.1038/bmt.2008.316.
[74] Perez-Simon JA, Lopez-Villar O, Andreu EJ, Rifon J, Muntion S, Campelo MD, et al. Mesenchymal stem cells expanded in vitro with human serum for the treatment of acute and chronic graft-versus-host disease: results of a phase I/II clinical trial. Haematologica 2011;96(7):1072–6. doi: https://doi.org/10.3324/haematol.2010.038356.
[75] Zhao AQ, Xie H, Lin SY, Lei Q, Ren WX, Gao F, et al. Interferon-gamma alters the immune-related miRNA expression of microvesicles derived from mesenchymal stem cells. J Huazhong Univ Sci Technol Med Sci 2017;37(2):179–84. doi: https://doi.org/10.1007/s11596-017-1712-1.
[76] Nie L, Li C, Zhao T, Wang Y, Liu J. LncRNA double homeobox A pseudogene 8 (DUXAP8) facilitates the progression of neuroblastoma and activates Wnt/beta-catenin pathway via microRNA-29/nucleolar protein 4 like (NOL4L) axis. Brain Res 2020;1746:. doi: https://doi.org/10.1016/j.brainres.2020.146947146947.
[77] Xu LJ, Yu XJ, Wei B, Hui HX, Sun Y, Dai J, et al. Long non-coding RNA DUXAP8 regulates proliferation and invasion of esophageal squamous cell cancer. Eur Rev Med Pharmacol Sci 2018;22(9):2646–52. doi: https://doi.org/10.26355/eurrev_201805_14959.
[78] Zuo R, Liu M, Wang Y, Li J, Wang W, Wu J, et al. BM-MSC-derived exosomes alleviate radiation-induced bone loss by restoring the function of recipient BM-MSCs and activating Wnt/beta-catenin signaling. Stem Cell Res Ther 2019;10(1):30. doi: https://doi.org/10.1186/s13287-018-1121-9.
[79] Huang P, Yan R, Zhang X, Wang L, Ke X, Qu Y. Activating Wnt/beta-catenin signaling pathway for disease therapy: Challenges and opportunities. Pharmacol Ther 2019;196:79–90. doi: https://doi.org/10.1016/j.pharmthera.2018.11.008.
[80] Djebali S, Davis CA, Merkel A, Dobin A, Lassmann T, Mortazavi A, et al. Landscape of transcription in human cells. Nature 2012;489(7414):101–8. doi: https://doi.org/10.1038/nature11233.
[81] Li F, Xiao Y, Huang F, Deng W, Zhao H, Shi X, et al. Spatiotemporal-specific lncRNAs in the brain, colon, liver and lung of macaque during development. Mol Biosyst 2015;11(12):3253–63. doi: https://doi.org/10.1039/C5MB00474H.
[82] Hon C-C, Ramilowski JA, Harshbarger J, Bertin N, Rackham OJL, Gough J, et al. An atlas of human long non-coding RNAs with accurate 5' ends. Nature 2017;543(7644):199–204. doi: https://doi.org/10.1038/nature21374.
[83] Marttila S, Chatsirisupachai K, Palmer D, de Magalhães JP. Ageing-associated changes in the expression of lncRNAs in human tissues reflect a transcriptional modulation in ageing pathways. Mech Ageing Dev 2020;185:111177. doi: https://doi.org/10.1016/j.mad.2019.111177.
[84] Herrera M, Llorens C, Rodríguez M, Herrera A, Ramos R, Gil B, et al. Differential distribution and enrichment of non-coding RNAs in exosomes from normal and Cancer-associated fibroblasts in colorectal cancer. Mol Cancer 2018;17(1). doi: https://doi.org/10.1186/s12943-018-0863-4.
[85] Lötvall J, Hill AF, Hochberg F, Buzás EI, Di Vizio D, Gardiner C, et al. Minimal experimental requirements for definition of extracellular vesicles and their functions: a position statement from the International Society for Extracellular Vesicles. J Extracell Vesicles 2014;3(1):26913. doi: https://doi.org/10.3402/jev.v3.26913.
[86] Phinney DG, Pittenger MF. Concise Review: MSC-Derived Exosomes for Cell-Free Therapy. Stem Cells 2017;35(4):851–8. doi: https://doi.org/10.1002/stem.2575.
[87] Börger V, Bremer M, Ferrer-Tur R, Gockeln L, Stambouli O, Becic A, et al. Mesenchymal Stem/Stromal Cell-Derived Extracellular Vesicles and Their Potential as Novel Immunomodulatory Therapeutic Agents. Int J Mol Sci 2017;18(7):1450. doi: https://doi.org/10.3390/ijms18071450.
[88] Wang K, Jiang Z, Webster KA, Chen J, Hu H, Zhou Yu, et al. Enhanced Cardioprotection by Human Endometrium Mesenchymal Stem Cells Driven by Exosomal MicroRNA-21. Stem Cells Transl Med 2017;6(1):209–22. doi: https://doi.org/10.5966/sctm.2015-0386.
[89] Ibrahim AGE, Li C, Rogers R, Fournier M, Li L, Vaturi SD, et al. Augmenting canonical Wnt signalling in therapeutically inert cells converts them into therapeutically potent exosome factories. Nat Biomed Eng 2019;3(9):695–705. doi: https://doi.org/10.1038/s41551-019-0448-6.
[90] Ma J, Zhao Y, Sun Li, Sun X, Zhao X, Sun X, et al. Exosomes Derived from Akt-Modified Human Umbilical Cord Mesenchymal Stem Cells Improve Cardiac Regeneration and Promote Angiogenesis via Activating Platelet-Derived Growth Factor D. Stem Cells Transl Med 2017;6(1):51–9. doi: https://doi.org/10.5966/sctm.2016-0038.
[91] Qu Y, Zhang Q, Cai X, Li F, Ma Z, Xu M, et al. Exosomes derived from miR-181-5p-modified adipose-derived mesenchymal stem cells prevent liver fibrosis via autophagy activation. J Cell Mol Med 2017;21(10):2491–502. doi: https://doi.org/10.1111/jcmm.13170.